Hastings on Hudson – Hydrodynamic Study Part 1 – Model Setup & Calibration

Stantec

Prepared for:
Atlantic Richfield Company
(a BP affiliated company)

Prepared by:
Stantec Consulting Services Inc.
30 Park Drive
Topsham, ME 04086

February 19, 2016

Sign-off Sheet

This document entitled Hastings on Hudson – Hydrodynamic Study Part 1 – Model Setup & Calibration was prepared by Stantec Consulting Services Inc. ("Stantec") for the account of Atlantic Richfield Company (a BP affiliated company) (the "Client"). Any reliance on this document by any third party is strictly prohibited. The material in it reflects Stantec's professional judgment in light of the scope, schedule and other limitations stated in the document and in the contract between Stantec and the Client. The opinions in the document are based on conditions and information existing at the time the document was published and do not take into account any subsequent changes. In preparing the document, Stantec did not verify information supplied to it by others. Any use which a third party makes of this document is the responsibility of such third party. Such third party agrees that Stantec shall not be responsible for costs or damages of any kind, if any, suffered by it or any other third party as a result of decisions made or actions taken based on this document.

Prepared by ______________________________________
(signature)

Brent Courchene
Associate

Prepared by ______________________________________
(signature)

Jeffrey Tabor, PE, D.CE
Senior Associate

Reviewed by ______________________________________
(signature)

Michael Chelminski, PE
Principal

Stantec

Table of Contents

LIST OF TABLES

LIST OF FIGURES

1.0 INTRODUCTION

The overall purpose of this study is to develop a hydraulic computer model that simulates baseline hydrodynamics in the Hudson River that are associated with the remediation design alternatives being consideration for a 28-acre site (Site) located in Hastings on Hudson, New York. The Site is situated along the eastern bank of the Hudson River, approximately 50 kilometers (km) (30 miles [mi]) upstream of its confluence with Upper New York Bay. This Site has a long history of industrial development dating back to the mid-1800s.

After initial review of available data and meetings with the client, it was determined that two models will be needed in order to capture the level of detail needed to evaluate the remediation designs under consideration for the Site. These include a coarse resolution regional hydrodynamic model of the Lower Hudson River (LHR Model) and a fine resolution local hydrodynamic model focused at the Site (HOH Model).

This document presents the information that was available and the processes used to develop, calibrate, and validate the LHR Model and also presents the initial HOH Model with example outputs from sample runs. This document also reviews forcing conditions and recommends an approach for modeling morphodynamic responses from long term seasonal forces and short term extreme events for post-construction conditions at the Site.

2.0 BOUNDARY CONDITIONS – RIVER DISCHARGE AND TIDE

The Lower Hudson River is a partially mixed, mesotidal estuary dominated by tidal currents with average velocities of 0.5 to 1 meters per second (m/s) (Nitsche et al. 2007). River discharge is highly seasonal with the maximum freshwater input during the snowmelt in spring and the major rainfall in autumn. Higher river discharge occurs during the spring freshet (~2,000 cubic meters per second [$m^3 s^{-1}$]) and lower discharge during the late summer (~200 $m^3 s^{-1}$). According to the United States Geological Survey (USGS) Station Number (No.) 01372058, daily river discharge and sediment flux closest to the Site is at Poughkeepsie, 75 km (46 mi) upstream from the Site. As shown in Figure 1, only of a small portion of the Hudson River watershed drains between Poughkeepsie and the Site (denoted by the red star). The accumulation of base and storm flows in the river between Poughkeepsie and the Site is assumed to be insignificant owing to this small sub-watershed.

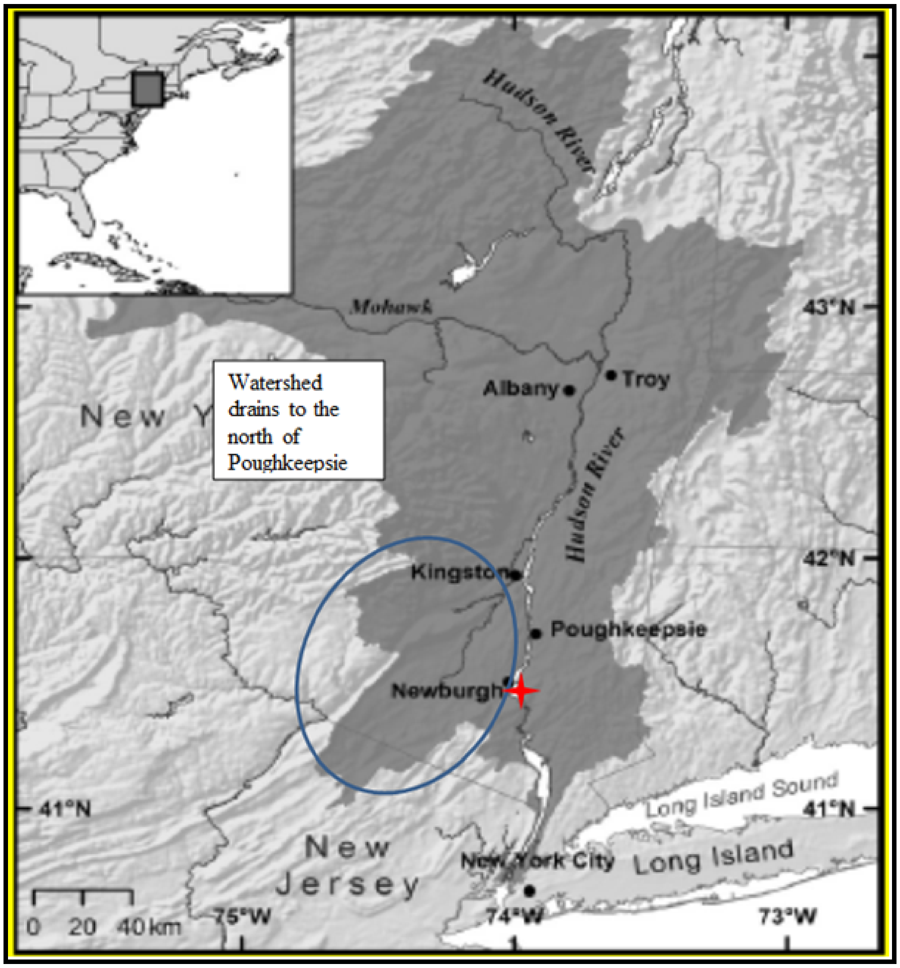

Figure 1: Hudson River Watershed

Further upstream, there is a longer historical record of river discharge at Green Island from USGS Station No. 01358000. A correlation analysis between flows at Green Island and Poughkeepsie on a monthly basis was established by comparing observed flows at Green Island and estimated flows at Poughkeepsie based on gaged and ungaged tributaries between Green Island and Poughkeepsie (Abood et al. 1992).

This relationship is given by:

$$Q_d = a + bQ_u$$

with:

Month	a	b
Jan	-413	1.477
Feb	-1179	1.600
Mar	4718	1.319
Apr	1115	1.311
May	-154	1.356
Jun	711	1.231
Jul	-12	1.228
Aug	-951	1.358
Sep	-192	1.237
Oct	-1968	1.569
Nov	-964	1.516
Dec	-958	1.421

where Q_d and Q_u are the discharges at Poughkeepsie and Green Island in ft^3s^{-1}, respectively. This empirical relationship can be used to obtain flow rates at Poughkeepsie for the length of record where such observations are made at Green Island but lacking at Poughkeepsie. Further, it shows the flow discharge from tributaries between Green Island and Poughkeepsie is not substantial relative to freshwater discharges from further upriver.

According to the studies performed at the Site by Ocean Surveys, Inc. (OSI) in 2001, the tide is characteristic of semidiurnal conditions. The wave length is about 160 km (550,000 feet [ft]) based on linear wave theory. This provides a rough estimate of spatial tide variation. Mean high water and mean low water are estimated to be at El. 2.2 ft and El. -2.0 ft (NAVD 88[1]) with a mean tidal range of 5.1 ft (1.6 m).

Tide data is available from several locations in the lower Hudson River. Figure 2 shows the locations of National Oceanographic and Atmospheric Administration (NOAA) and USGS water level and discharge stations. The NOAA sources include a long history of observed water levels/tides at the Battery on Manhattan Island (NOAA 8518750), as well as two others closer to the site, which contain model predictions of daily tides. Those model predictions fail to capture the non-astronomical components of tidal water levels and are, therefore, inferior to actual observations.

[1] North American Vertical Datum of 1988

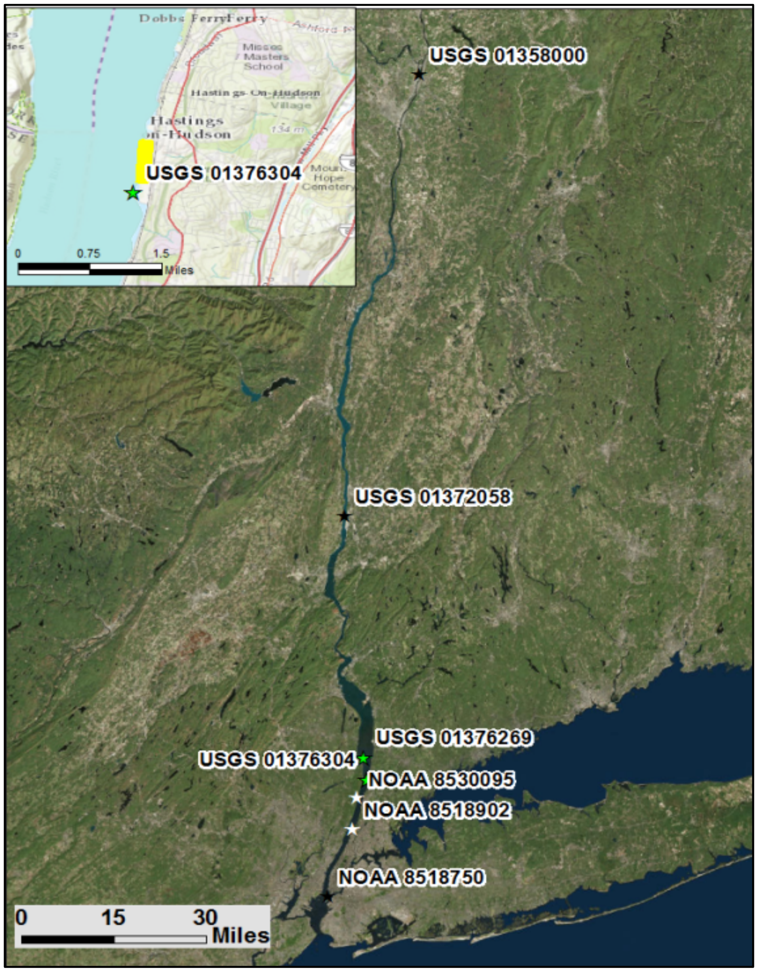

Figure 2: Water Level and Discharge Gages

The USGS also has observations of water levels. These data are recorded at 15-minute intervals and other investigations have utilized hourly water levels from these stations for modeling purposes (Ding and Wang 2006). Data from these gages have been obtained and used for validating modeled water levels at the Site. Table 1 provides a list of gage locations and length of observations.

Table 1: Observation locations in Lower Hudson River

Site ID	Tide (yrs)	Discharge (yrs)	Sediment Flux (yrs)	Description
USGS 01376304	1992–2010			south end, daily
USGS 01358000		1946–2010		200 km (125 mi) upstream, daily
USGS 01376269	2010–2015			6 km (4 mi) upstream, daily
USGS 01372058	2002–2011	1992–2015	2002–2011	75 km (46 mi) upstream, daily
NOAA 8518750	1920–2015			50 km (31 mi) downstream, hourly prediction, observation
NOAA 8518902	2013–2015			14 km (9 mi) downstream, hourly prediction, harmonic
NOAA 8530095	2013–2015			6 km (4 mi) downstream, hourly prediction
[2]**USGS 01372500**		1928–2015		Wappinger Creek, daily
[1]**USGS 01375000**		1933–2015		Croton Creek, daily

River discharge and water level represent the required upstream and downstream boundary conditions required in modeling the hydrodynamics of a tidal river, respectively. Given that flow discharge from tributaries between Poughkeepsie and Green Island is relatively small and the most long term observed discharge record exists at Green Island, it has been determined that the upstream boundary of the LHR model will be located at this location.

While there are time series of observed water levels closer to the site at USGS Station No. 01376304 and 01376269, the time series of water level at the Battery (NOAA 8518750) has been selected as the location and source for the downstream boundary owing to its longer recording history. The main purpose of the LHR Model is to provide forecasting/hindcasting of hydrodynamic forcing for boundary conditions of the HOH Model. Therefore, validation and calibration of the LHR Model is appropriate. Maintaining observations within the modeling domain (i.e., water levels at USGS Station No. 01376304 and 01376269) and near the Site allow for this validation and calibration.

3.0 SOURCES FOR MODEL CALIBRATION AND VALIDATION

3.1 CURRENTS

The flow information collected by OSI in 2001 indicated that peak flood currents typically occur during the peak stage in the cycle and peak ebb currents typically occur at the minimum stage. Measured surface current speeds at distances 100 to 500 ft west of the existing western shore of the Site were typically highest north of the North Boat Slip, with peak ebb-tide velocities of 4.0 ft per second (fps) and peak flood-tide velocities of 3.5 fps. Velocities were found to be typically lower closer than 100 ft to the existing shore and were typically lower near the river bottom. Below the surface, maximum current velocities were observed to be up to 2.3 fps near the channel bottom in the zone 100 to 500 ft offshore. Independent of depth, maximum velocities within 100 ft of the existing shore were found to be near 2.0 fps (Earth Tech 2003). In addition to

[2] Tributaries, not shown on map

these observations of tidal current velocities near the Site, several sources of current measurements and predictions are available for model validation and calibration.

There were several locations of depth-dependent current velocity profiles measured by NOAA during the Hudson River 2005/2006 Current Surveys. Table 2 and the accompanying map (Figure 3) show the locations of these measurements and duration over which records were collected.

Table 2: NOAA Hudson River Current Survey Locations and Durations

Station Name	Deployed	Recovered
Mid-Hudson Suspension Bridge (MHSB)	9/21/2006 18:31	11/1/2006 15:29
Roseton (RST)	8/24/2005 18:07	10/19/2005 20:35
Newburgh Beacon Bridge (NBB)	7/7/2005 13:40	8/23/2005 21:40
Bear Mountain Bridge (BMB)	7/7/2005 0:40	8/23/2005 18:40
Stony Point (SPT)	7/6/2005 23:08	8/23/2005 17:45
Haverstraw (HVW)	6/8/2004 14:14	7/28/2004 14:20
Tappan Zee Bridge (TZB)	6/2/2005 17:12	7/6/2005 20:17
George Washington Bridge (GWB)	8/14/2006 15:15	11/1/2006 22:51
George Washington Bridge (GWB)	6/2/2005 14:54	7/6/2005 17:05
George Washington Bridge (GWB)	4/4/2006 16:40	6/21/2006 18:21
George Washington Bridge (GWB)	7/6/2005 17:59	9/2/2005 17:50
Gowanus Flats LBB 32 (GFL)	2/25/2013 12:00	5/27/2013 0:00

In addition to these NOAA data, a side mounted Acoustic Doppler Velocity Meter has been recording stream velocities at the USGS Poughkeepsie station (Station No. 01376269) since August 23, 2015.

The final source of observed current velocities was from Acoustic Doppler Current Profile (ADCP) measurements recorded for the 'Hudson River Currents, Mixing and Sediment Transport' research project at Colombia University. Data were measured for several months during 2002, 2003, and 2004 (detailed in Table 3). However, these data are not available for the public use.

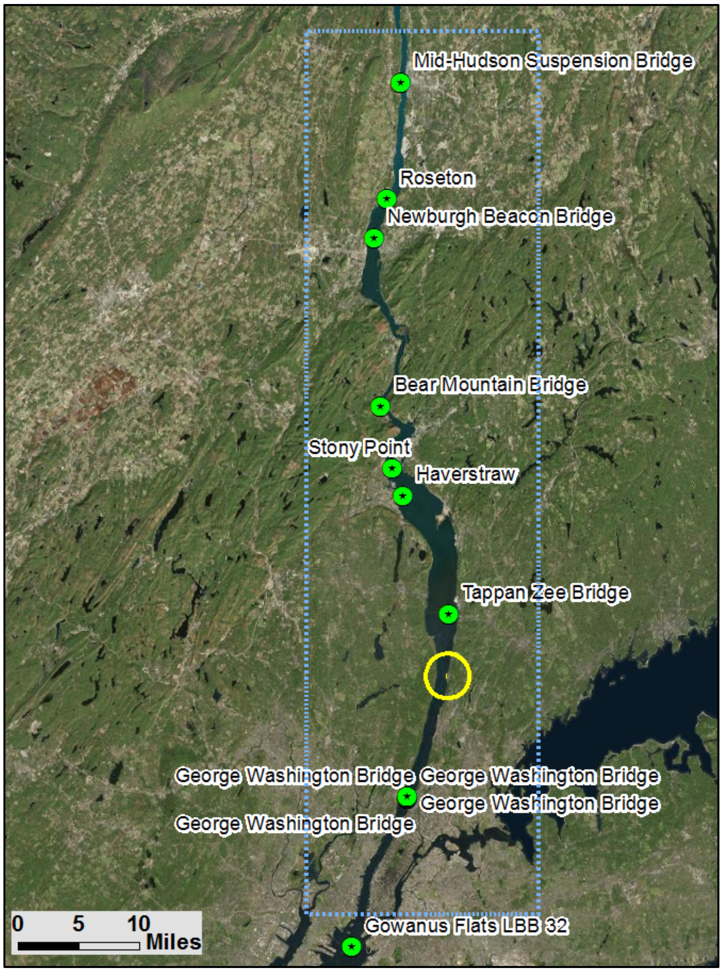

Figure 3: LHR Model extent (blue) in relation to the Site (yellow)

Table 3: Location and Dates of ADCP Measurements by Columbia University

Station Name	Deployed	Recovered
N. of George Washington Bridge	05/21/02	05/28/02
near Kingston, NY	07/22/03	07/31/03
off Piermont Pier, Piermont, NY	11/24/03	12/03/03
off Piermont Pier, deep channel	03/25/04	05/07/04
upper Haverstraw Bay, deep channel	03/24/04	05/07/04
off Piermont Pier, deep channel	05/13/04	07/12/04
upper Haverstraw Bay, deep channel	05/12/04	07/03/04

Along the study area, tidal currents are dominant (Nitsche et al. 2007). Therefore, NOAA predicted tidal velocities are a good representation of actual channel velocities. Predicted tidal currents for different stations along the Hudson River (Figure 4) are available through NOAA tide/currents for 2010–2015. Predictions include 4–5 current values for each day at flood, ebb, and slack water times.

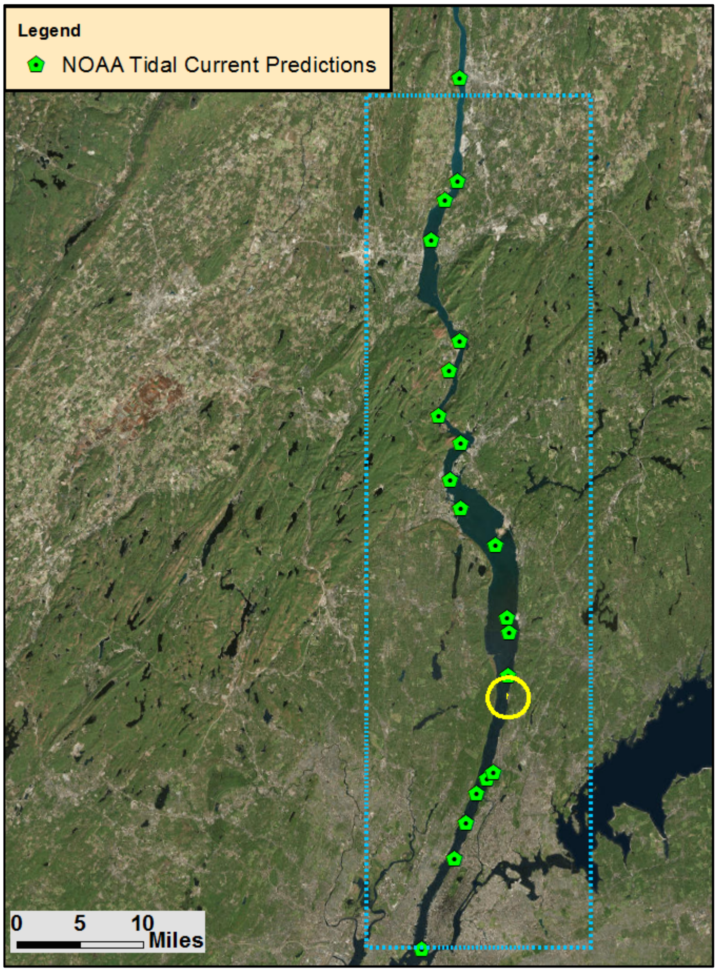

Figure 4: Location of NOAA Tidal Current Predictions

3.2 WATER QUALITY

The Hudson River is a partially mixed estuary with the salinity intrusion ranging between 30 and 120 km upstream from the Battery, depending on river discharge and tidal forcing. Based on the salinity, conductivity, temperature, and turbidity measurements performed by OSI at the site, the water column at the Site is well mixed with minimal density-stratification and no well-defined salt wedge.

An extensive set of salinity observations was completed during spring and summer 2004 when seven moorings were deployed along the channel from the Battery (river km 0) to Bear

Mountain (river km 75) (Ralston et al. 2008). This study identified salinity variations between 0 to 10 practical salinity units (psu) at the Site.

Another source of water level, salinity, and turbidity data is available from the Hudson River Environmental Conditions Observing System (HRECOS). These records of observations date back to 2008. Additional salinity data was obtained from the database provided for supporting the New York Harbor Observing and Prediction System (NYHOPS). Figure 5 shows the locations of the HRECOS and NYHOPS stations. Salinity, water level, and turbidity data from HERCOS and NYHOPS data bases are tabulated in Table 4.

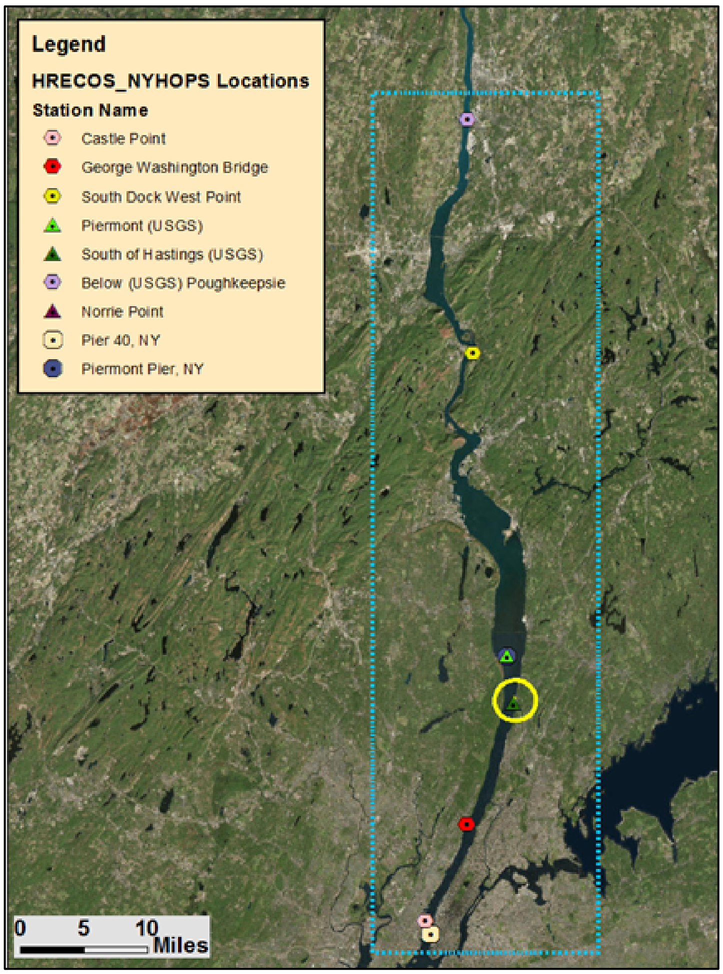

Figure 5: Location Map of HRECOS and NYHOPS Stations

Table 4: Types of Data and Length of Record for HRECOS and NYHOPS Stations

Station Name	Observation	Period
Pier 40, NY	Salinity, Water Level, Atmospheric	2007–2010
George Washington Bridge	Salinity, Water Level, Atmospheric, Water Surface Temperature	2008–2012
South of Hastings (USGS)	Salinity, Water Level, Water Surface Temperature	2007–2010
Piermont Pier, NY	Salinity, Turbidity, Water Surface Temperature	2008–2015
Piermont (USGS)	Salinity, Water Level, Water Surface Temperature	2010–2015
Castle point, Buoy1	Salinity	2008–2012, 2014, 2015
Castle point, NY	Water Level	2006, 2008
Norrie Point	Salinity, Turbidity	2008–2013
South Dock West Point	Salinity, Turbidity, Water Surface Temperature	2013, 2014
Below (USGS) Poughkeepsie	Salinity, Turbidity, Water Surface Temperature, Atmospheric	2007–2015

In addition to continuous time series of salinity and turbidity mentioned above, data are available from the Riverkeeper Water Quality Program (Riverkeeper). This program aims to improve the water quality of the Hudson River and its tributaries through increased water quality monitoring and public notification, consistent investment in wastewater and stormwater infrastructure, and better water quality policies. Riverkeeper monitors water quality on the Hudson River Estuary in collaboration with scientists from Columbia University's Lamont-Doherty Earth Observatory and Queens College, CUNY. Riverkeeper tests for fecal-indicating bacteria, oxygen, turbidity, temperature, salinity, and chlorophyll at a vast number of stations throughout the river from upstream of Green Island down to the river mouth at Battery. Among all the physical/chemical data collected by Riverkeeper, salinity and turbidity are the most useful for model validation/calibration purposes.

This Riverkeeper record is available from the beginning of 2006 to the present. Water quality parameters have been recorded at different stations during the past 9 years. The recording is not continuous and mostly takes place during the high flow conditions on specific days. At different stations the total number of samples during the recording years varies. Samples are taken from approximately 30 centimeters below the water surface. The sampling dates are known but the exact time is not reported. Although the sampling does not have a continuous history of water quality information, the numerous stations during 9 years of record are useful for LHR Model validation/verification purposes.

3.3 SEDIMENT

The confluence of the Mohawk and Upper Hudson Rivers is 250 km upstream from the Battery. It is estimated that these rivers supply between 0.2 and 1.0 million metric tons (MT) of sediment annually to the Lower Hudson River. During spring freshets with moderate to high discharge, sediment flux is down-estuary and sediment deposits downstream of the Site in in New York Harbor. In the summer months after the spring freshet, sediment flux is up-estuary. During relatively low-discharge freshets, sediment flux may be persistently up-estuary because baroclinic trapping remains strong (Ralston et al. 2008).

The closest daily sediment discharge observations to the Site are collected at USGS Station No. 01372058 located 75 km (46 mi) upstream in Poughkeepsie (Figure 2). This discharge is used as an upstream boundary condition for morphodynamic modeling in the LHR Model.

The sediment type and sedimentary environments along the entire Hudson River estuary are shown in Figure 6. These data were obtained from the New York State GIS Clearinghouse (NYGIS). Reference Nitsche et al. 2007 for details of these dataset. The corresponding physical properties of these sediments are listed in Table 5 (Ralston et al. 2012). These data will be used to parameterize the morphodynamics of the LHR Model. Laboratory testing of sediment grain size with samples collected near the site was provided. Results indicate the median sediment size (D_{50}) near the Site is approximately 0.01 mm, which is a silt-size classification.

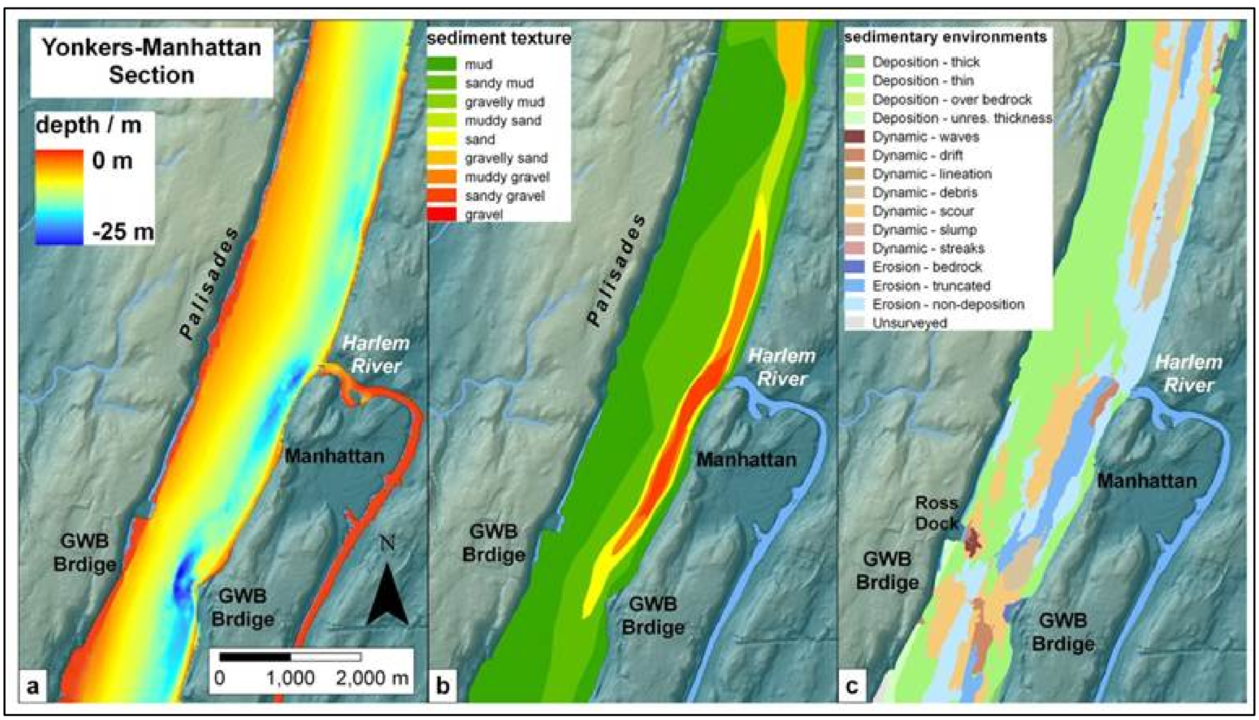

Figure 6: Sediment Types in Section of Lower Hudson River (cited from Nitsche et al. 2007)

Table 5: Physical Properties of Sediment Types (Ralston et al. 2012)

Sediment Class	Settling Velocity ($mm\ s^{-1}$)	Erosion Rate ($kg\ m^{-2}\ s^{-1}$)	Critical Stress for Erosion ($N\ m^{-2}$)
Medium sand (bed)	40.	$1*10^{-4}$	0.5
Fine sand (bed)	5.	$1*10^{-4}$	0.1
Silt (bed)	0.6	$1*10^{-4}$	0.05
Silt (River)*	0.1,0.6	$1*10^{-3}$, $1*10^{-4}$	0.05
*Properties where salinity < 0.5 psu (practical salinity unit). Sediment from the river has a slower settling velocity and higher erosion rate in fresh water to represent unflocculated particles, and it has properties equal to the silt fraction of the bed where salinity > 0.5 psu			

3.4 BATHYMETRY

Site bathymetry data collected during a 2012 OSI survey was provided by Haley and Aldrich in the form of an AutoCAD file. The along shore extent of this survey was approximately 600 ft north and 500 ft south of the Site property boundaries. This extent captures the old marina area to the north and the northern most mooring dolphin south of the Site as well as all features along the shoreline. The survey extends approximately 650 ft to 700 ft west into the Hudson River from the Site.

The bathymetry contours were imported into ArcGIS and a triangulated irregular network (TIN) was created using these contours. Additional processing was performed to create a point shapefile at the TIN nodes. From these nodes, a xyz depth file was created in a format required for modeling in Delft3D. All projections were converted from state plane feet to geographic coordinates and vertical units were converted from feet to meters. Figure 7 shows the TIN that was created from the bathymetry survey contours for use in the Delft3D grid development.

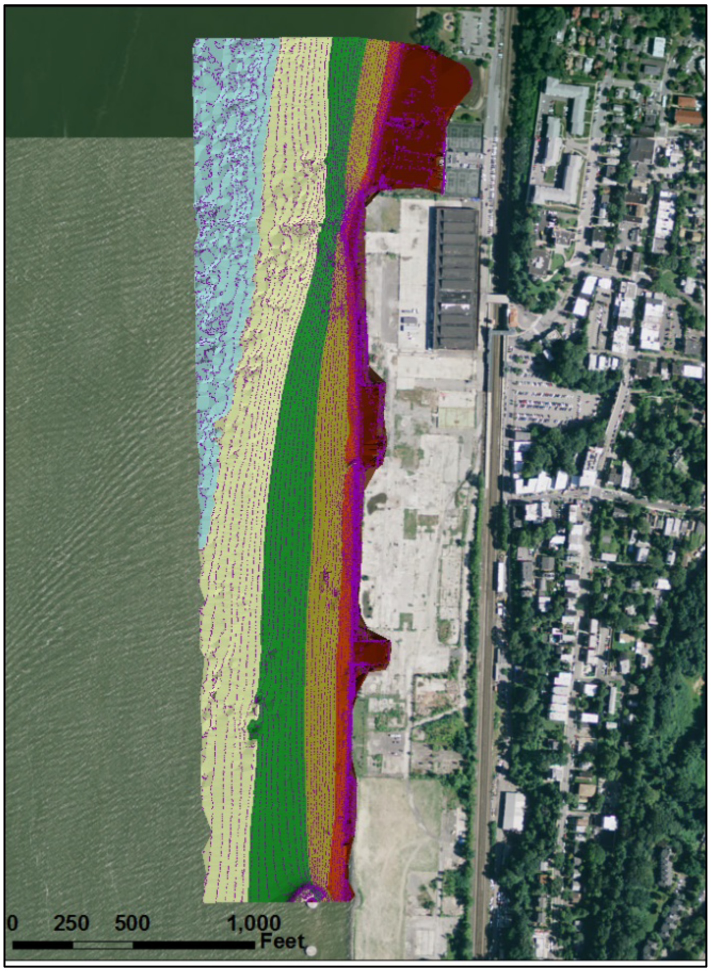

Figure 7: The TIN (color scale) created from the 2012 bathymetry survey contours

Beyond the extent of the 2012 bathymetry survey, 1-meter contours at a 10-meter horizontal resolution were used to create a TIN and xyz depth file. These contours originate from multibeam bathymetry surveys performed as a part of the Hudson River Benthic Mapping Project. The survey dates used to produce this complete survey set range from 1999 to 2003. Care was taken to remove the area from this data set, which overlaps with the 2012 site OSI survey as it is assumed that the 2012 site survey is of higher accuracy.

The 1-meter contours do not span the entire width of the river. To complete the bathymetry data for the Delft3D grid that is not covered by the 2012 OSI survey or the contours, the Hudson River Estuary Bathymetry 30-m grid was used. Figure 8 shows the three bathymetry sources near the Site. The red, blue, and gray color scales represent the coverage of the 2012 OSI survey, 1-m contours, and 30-m grid, respectively.

Figure 8: Available Bathymetry for the model

3.5 TOPOGRAPHY

Elevation data along the banks of the river were obtained in order to model hydrodynamics when the river is at various flood stages. The elevation was derived from two sources. Along either bank of the river, from roughly 1.5 miles north of to 1.5 miles south of the Site, elevations were derived from the 2011–2012 New York State Department of Environmental Conservation LiDAR: Coastal New York (Long Island and along the Hudson River) database. To the north and south of this extent, elevations derived from the USGS national elevation dataset (NED) were obtained. The resolutions of these data sources are sub meter and approximately 10 m (1/3 arc-second), respectively. Figure 9 shows the sources of topography data used.

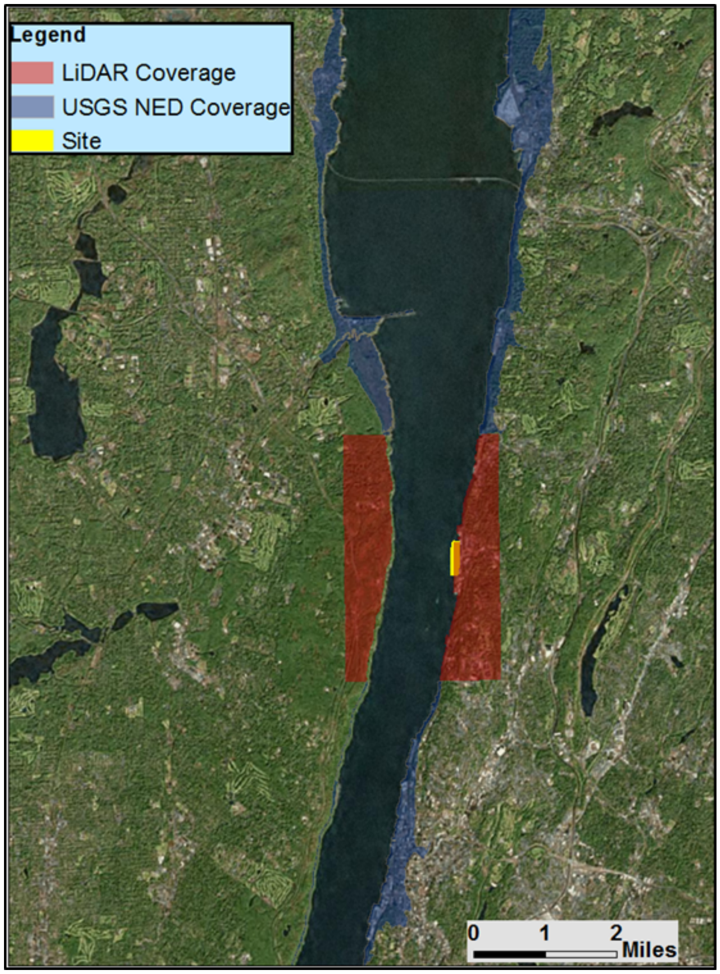

Figure 9: Topographic Sources Near the Site

4.0 LHR MODEL GRID DEVELOPMENT AND CALIBRATION

4.1 COMPUTATIONAL MESH

As described, two model grid settings have been generated: 1) a coarse regional mesh from Green Island to the Battery (LHR Model); and 2) a fine local mesh focusing on the Site as well as the upstream and downstream areas within its immediate vicinity (HOH Model). The LHR Model will be used to develop boundary conditions for the HOH Model and is described herein.

The LHR Model, covering the Lower Hudson River from Green Island in the north to the Battery in the south, is developed based on a regular curvilinear grid form. The boundary of the LHR Model follows the general banks of the Hudson River and includes boundaries for Pollepel Island, Iona Island, Round Island, and Con Hook. A spherical coordinate system is applied for the grid generation, setup, and modeling. A combination of the NOAA, USGS and the bathymetry contour lines discussed in Section 3 were used to create a seamless topographic/bathymetric dataset. This seamless dataset was converted to 50m X 50m xyz sample data, which is required by the Delft3D grid generator module. Figure 10 illustrates the generated grid, depth and mesh orthogonality, respectively from left to right.

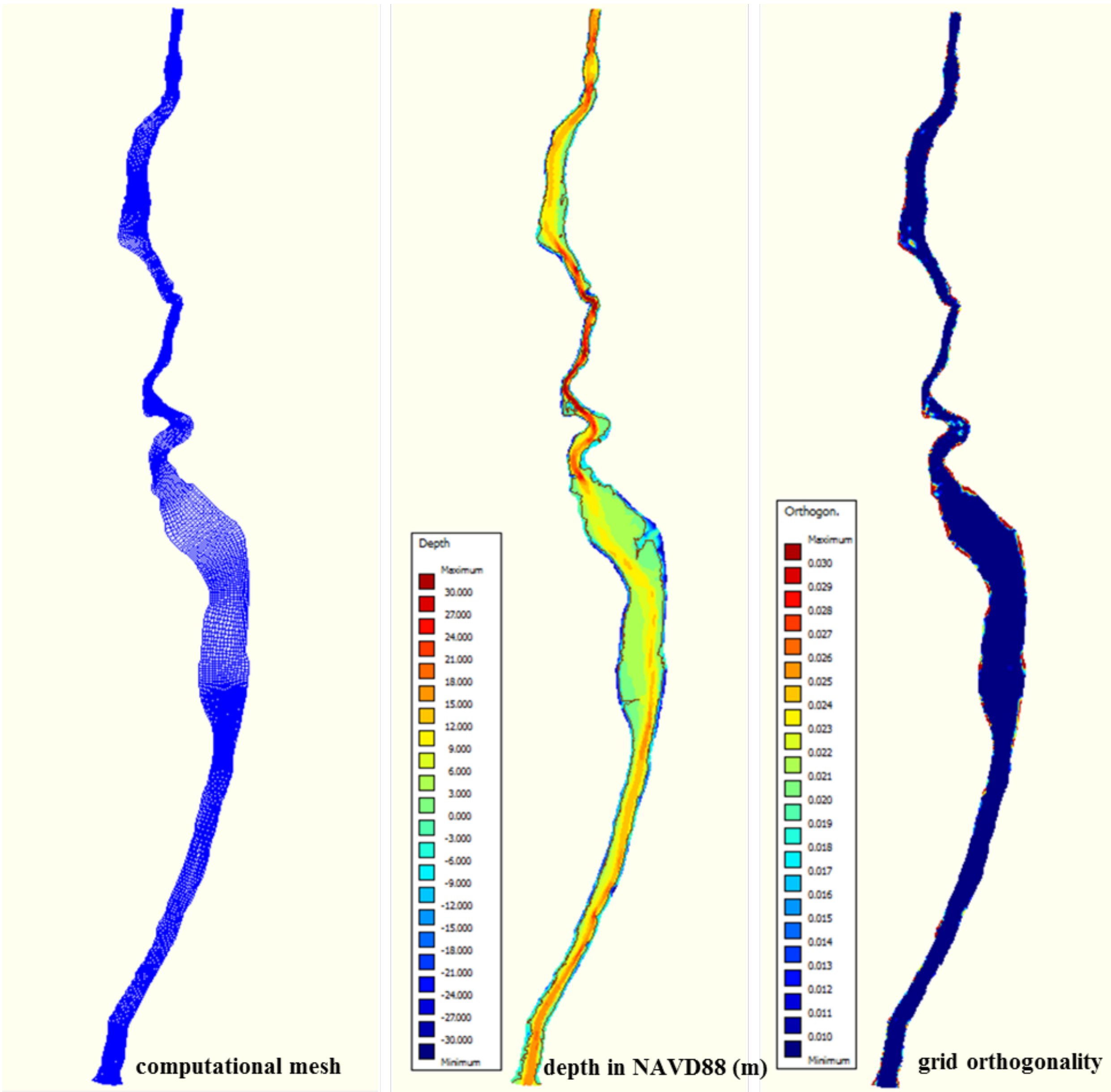

Figure 10: LHR Model grid development from Battery to Poughkeepsie

Figure 11shows the grid size becoming finer approaching the Site. In addition to the Site, the grid size decreases where higher resolution is required to resolve Hudson River geometry/features, such as bends, complex banks, and small islands or bays.

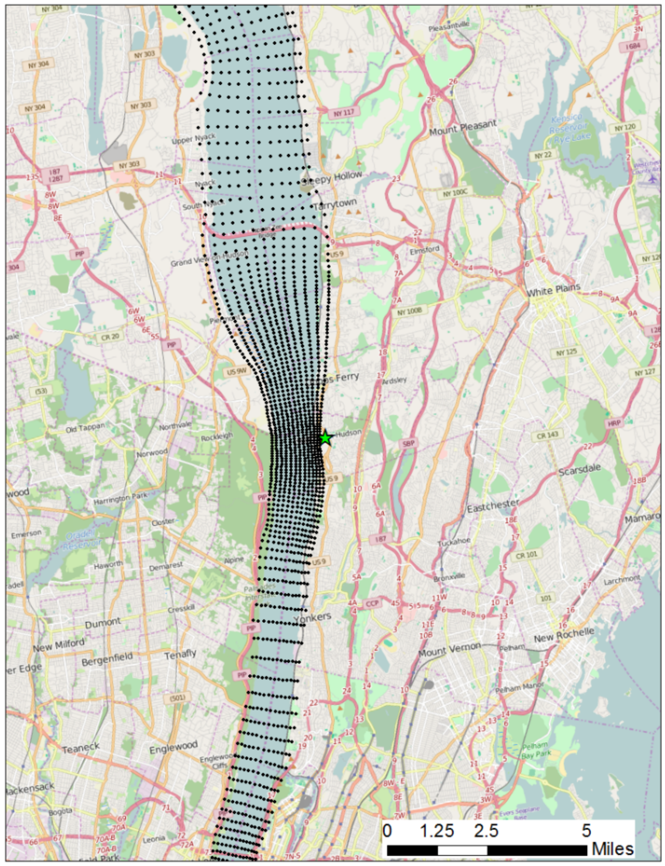

Figure 11: LHR Mesh size decreases locally at the Site (Denoted by the Green Star)

The along river extent of the LHR Model domain is from The Battery to Green Island as described in Section 2. The goal of the LHR Model is to be fine enough to attain accurate predictions of hydrodynamic forcing near the Site with the ability to run long-term simulations within a reasonable amount of time. Six (6) separate models with different levels of mesh refinement were developed to perform an analysis to select a final mesh that is expected to provide suitably accurate simulations at the Site when executing long term simulations. Table 6 presents the number of cells in along and across the River as well as the total number of cells for each of these candidate meshes.

Table 6: Number of cells and grid resolution for all 6 candidate grids

Grid Name (Level of resolution)	Number of Cells Along the River	Number of Cells Across the River	Total Number of Cells	Finest Cell Size at Hasting (m)
Coarsest	342	6	2052	200
Coarse	570	9	5130	160
Mid-Coarse	430	12	5160	110
Mid	798	15	11970	90
Fine	1026	18	18468	75
Finest	1254	24	30096	50

The model sensitivity to the mesh size is being termed a convergence analysis because the aim is to identify where modeled results converge as grid size reduces. Comparison of hydrodynamic parameters from each of the candidate grids were done to determine the resolution at which further refinement would lead to negligible changes. The modeling grid at which convergence is realized has been used to carry forward for validation and calibration and represents the final LHR Model grid recommendation. Again, each level of mesh refinement features a mesh with a varying degree of resolution along the Hudson River with the finest resolution near the Site and in Hudson River bends. The finest and coarsest model grids assessed had approximate resolutions of 50 and 200 m near the Site, respectively (see Table 6).

4.2 LHR CONVERGENCE ANALYSIS RESULTS

In order to test the sensitivity of the LHR Model grid size, a 30-day simulation was performed using observed tides at the Battery and Hudson River discharge at Poughkeepsie from February 1, 2015, to March 3, 2015. In each of the six candidate model grids, four observation cells were selected: one near the upstream end, one near the Tappan Zee Bridge (TZB) just upstream of the Site, one in the main channel adjacent to the Site, and the last near the downstream end. The time series of water levels and horizontal velocity components (north-south, V and east-west, U) produced by each 30-day simulation were compared. The water levels at each observation location were also compared but proved to be relatively insensitive to the model resolution. Velocity is an important parameter given that shear stress is proportional to the square of the velocity and sediment transport to its cube; comparisons between velocity (U and V) are therefore presented in support of the selection of a preferred modeling mesh.

Review of the V time series (Figure 12) reveals that the differences between modeled results are quite small at the location nearest to the Site with the exception of the Coarsest resolution model, indicating low sensitivity to mesh size at these scales. The bottom plot however reveals that there is convergence at the Mid-Coarse resolution scale. This indicates little accuracy is expected to be gained by running a grid finer than the Mid-Coarse resolution model at these scales.

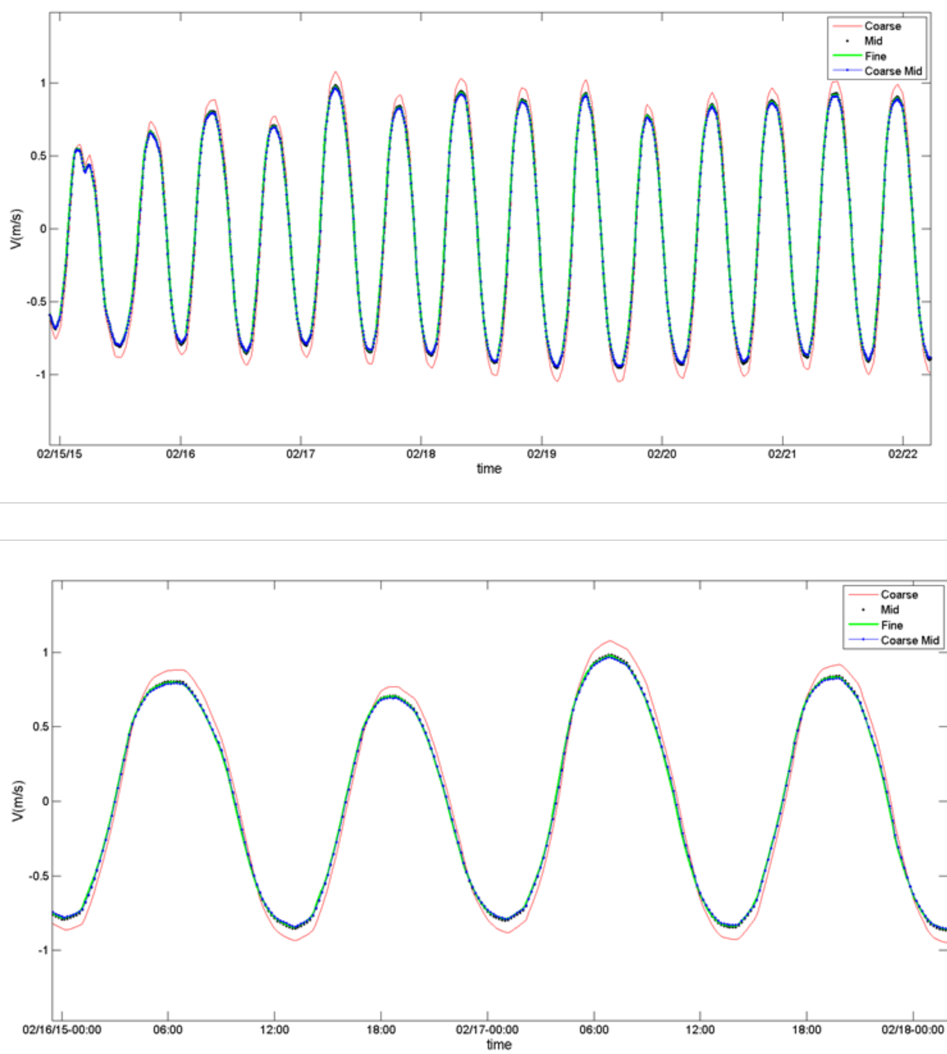

Figure 12: Time series of V-component of current velocity at Site from 2/15–22/15 (top) and 02/16–18/15 (bottom)

Table 7 shows the average, maximum, and standard deviation of the percent difference at peak velocity between each model prediction of depth averaged current velocity at the comparison location adjacent to the Site and that predicted by the finest resolutions model. This provides quantitative evidence that model refinement beyond the Mid-Coarse resolution model will have negligible impact on results of model simulations.

Table 7: Difference between peak current velocities at the Site as predicted by various grid resolutions

	Coarsest	Coarse	Mid-Coarse	Mid	Fine
Mean	15.1%	10.6%	1.0%	1.1%	0.3%
Standard Deviation	2.7%	1.6%	0.8%	0.6%	0.3%
Maximum	20.9%	16.5%	5.3%	3.8%	1.8%

One note pertaining to this convergence analysis is that full convergence is not to be expected. The results that are compared come from the center of a select mesh cell. Based on the different resolutions, these locations do not lie exactly on top of one another. Figure 13 shows a comparison of the exact locations of the observations near the TZB and the Site for the Coarsest, Mid, and Finest resolution models. Some of the differences in simulated results may come from this fact and will account for only a small percentage of differences summarized in Table 7. Consequently, the recommendation to proceed with the Mid-Coarse mesh is warranted.

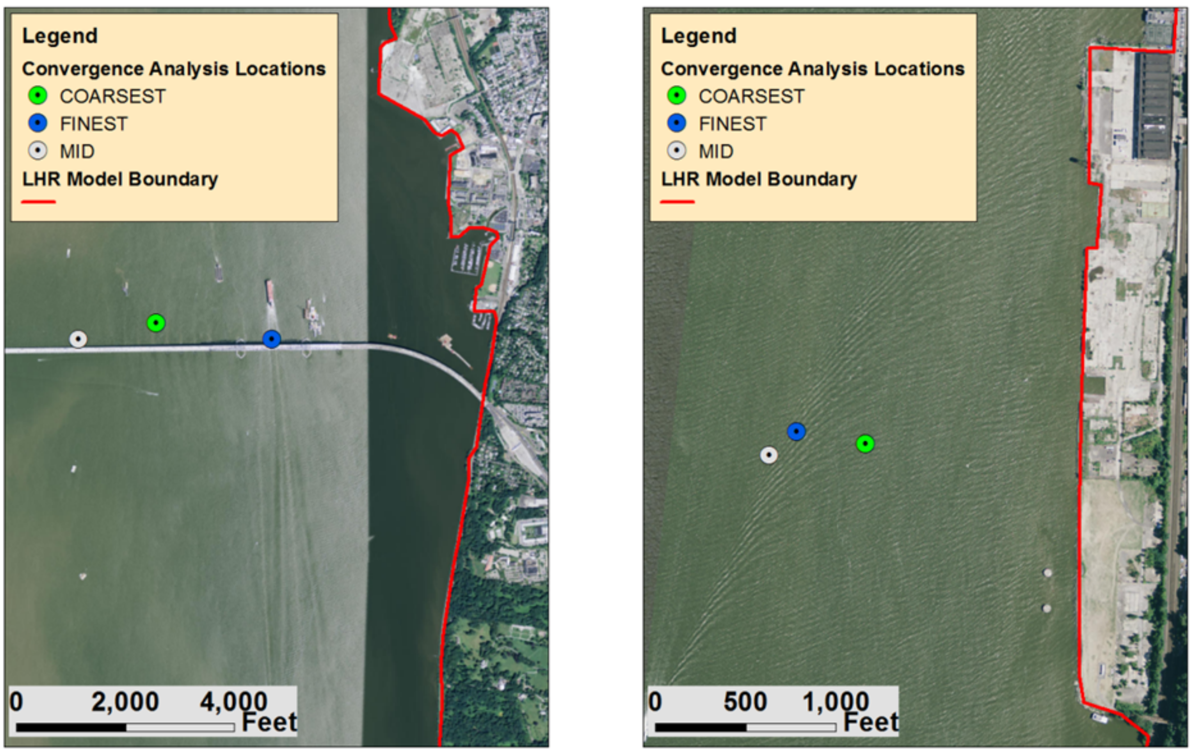

Figure 13: Locations of observations for time series comparisons at TZB (left) and the Site (right)

4.3 LHR PERFORMANCE ANALYSIS RESULTS

To assess the tradeoff between model convergence and model runtime, a performance analysis was also conducted. The Finest, Mid-Coarse, Coarse, and Coarsest resolution models were rerun including salinity and a steady, uniform wind. The runtimes of the convergence analysis runs can be compared (Table 8) to assess the marginal computation times required for model simulations based on grid size. Comparing the runtimes of each grid with and without salinity (Table 9) and wind can provide an estimate for the marginal increase in model simulation time associated with including more physical parameters.

Table 8: Simulation times for all proposed grids

Grid Name (Level of resolution)	Wall Clock (s)	Momentum Eq. (s)	Continuity Eq. (s)	Transport (s)	Turbulence (s)	Simulation duration (days)	Simulation Speed (hrs/Day)
Coarsest	5502	2054	1789	0	90	30	0.05
Coarse	9544	3672	3175	0	144	30	0.09
Mid-Coarse	12705	4820	4125	0	204	30	0.12
Mid	24554	10585	7620	0	325	30	0.23
Fine	52903	24435	16035	0	676	30	0.49
Finest	90027	42043	27264	0	1149	30	0.83

Table 9: Simulation times for proposed grids including salinity and wind

Grid Name (Level of resolution)	Wall Clock (s)	Momentum Eq. (s)	Continuity Eq. (s)	Transport (s)	Turbulence (s)	Simulation duration (days)	Speed (hrs/Day)
Coarsest	2060	426	370	276	567	7	0.08
Coarse	9804	2122	1780	1296	2592	14	0.19
Mid	46597	12379	8250	6070	11271	30	0.43
Finest	33401	9341	5906	4480	7730	7	1

The Mid-Coarse model was evaluated through an iterative process of realizing model convergence while maintaining high speed production with the ability to model long-term simulations. Therefore, the Mid-Coarse grid has been selected as the LHR Model mesh and was used in calibrations to finalize the LHR Model.

4.4 LHR MODEL CALIBRATION/VALIDATION

4.4.1 Current Velocity/Water Level

The LHR Model was calibrated based on best observational data available. Hourly time series of observed water level close to the Site is available from 1992 to 2010 at USGS Station No. 01376304. For current data, NOAA recorded vertical current velocity profiles at several locations in the Hudson River over different durations during 2005 and 2006, most of which covers June and July 2005 were used. The corresponding depth averaged velocity in June to July, as well as water level data at USGS Station No. 01376304, were used for model calibration. According to a brief literature review, the Hudson River has manning coefficients (n-value) ranging from 0.01 to 0.025 in most applications (Wang et al. 2014). The model parameter that can be adjusted for calibration purposes is the n-value. Table 10 below indicates the model sensitivity to this n-value across the typical range applied in the Hudson River. In Table 10, the percent difference between velocity magnitudes as well as between water levels at tidal peaks (high and low tide) for various n-values relative to an n-value of 0.015. Based on the sensitivity of velocity and water levels to n-value, the n-values applied in the final LHR model vary spatially to achieve strong model/observation agreement.

Table 10: Comparison of peak current velocities and high and low tide water levels for various n-values relative to an n-value of 0.015

	Current Velocity		Water Level	
	n-value = 0.020	n-value = 0.025	n-value = 0.020	n-value = 0.025
Mean	15.1%	33.4%	10.9%	18.1%
Standard Deviation	7.4%	12.4%	3.1%	5.1%
Maximum	25.0%	41.2%	20.6%	33.0%

To achieve the initial calibration of the LHR Model, the period from June to late October 2005 was simulated. The simulated time series of water levels at USGS Station No. 01376304, magnitude, and direction of the depth averaged velocity at George Washington Bridge (GWB), TZB, and Stoney Point (SPT) are compared with the corresponding measurements, which show a good agreement. To assess the calibration of the model quantitatively against the measured water level, current time series, the Nash-Sutcliffe (N-S) efficiency coefficient (E) is employed, where E is defined as:

$$E = 1 - \frac{\sum_{i=1}^{N}(X_{obs} - X_{mod})^2}{\sum_{i=1}^{N}(X_{obs} - \overline{X_{obs}})^2}$$

where X_{mod} is the modeled data, and X_{obs} is the measured data with $\overline{X_{obs}}$ the mean value. The simulated water level close to the site is in near-perfect agreement with the measurements with E=0.97. The magnitude of the simulated velocity at GWB, TZB, and SPT have the N-S efficiency coefficient E=0.96, 0.91, 0.92, and 0.95, respectively, which indicates strong agreement at all locations. It is further noted that the simulated current closest to the site has strong agreement with the measurements. Figure 14 shows the comparison between simulated time series of water level and velocity at all observation locations.

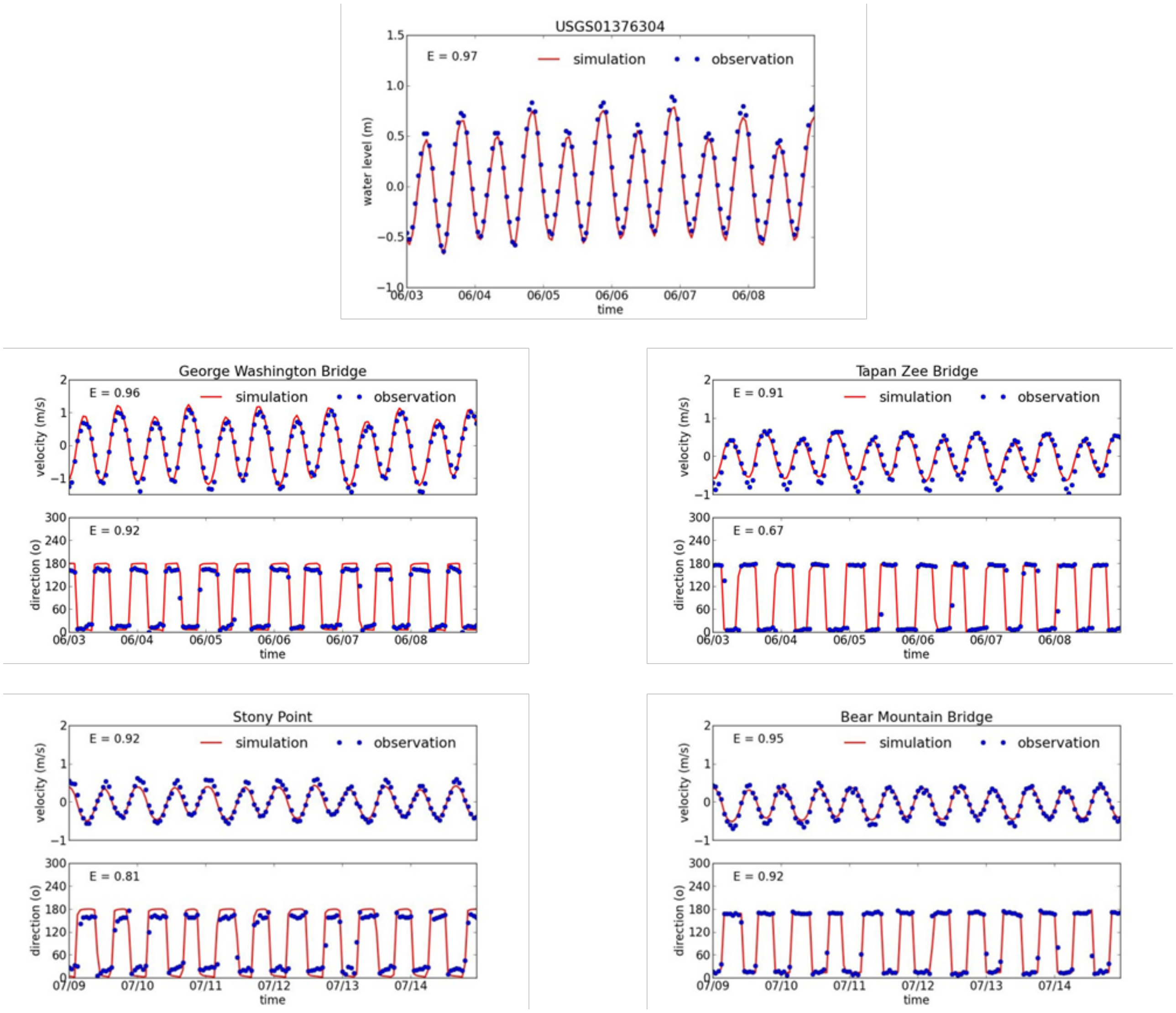

Figure 14: Comparison of Model Results and Observations for a Segment of the June–October 2005 Simulations. (top) Water Level at USGS 01376304 (bottom from left to right, top to bottom) Velocity at GWB, TZB, SPT, and BMB

To evaluate that the model is not calibrated to these particular locations at these particular times, additional model predictions were made for a period from Jan to late July 2011. While observations of current velocities are unavailable during this time period, there are two different stations of water level data (Piermont Pier [PPR] [USGS U01376269] and GWB). The simulated results for this period also show near-perfect agreement with observations (see Figure 15) based on the calculated efficiency coefficients of E=0.97 and E=0.98 for GWB and PPR, respectively.

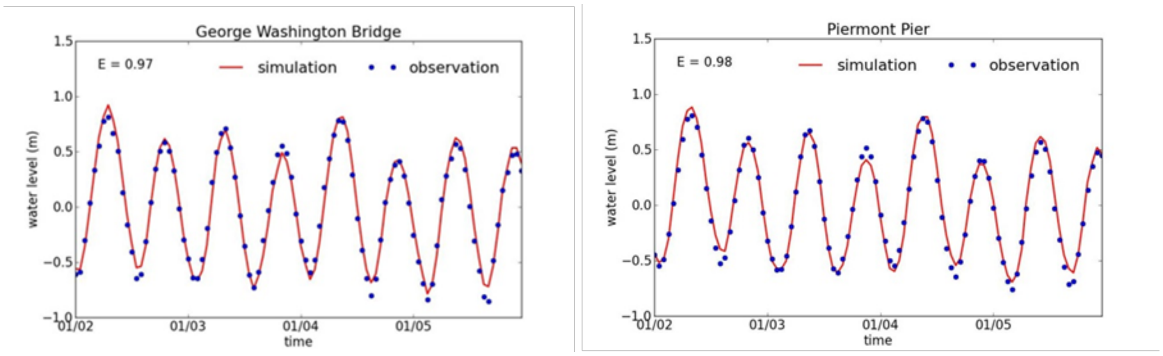

Figure 15: Comparison of Model Results and Observations for a Segment of the May–July 2010 Simulations. Water Level at the GWB (left) and at USGS 01376269 (right)

4.4.2 Salinity

The salinity calibration is based on available data from HRECOS. Hourly time series of salinity at Castle Point (CPT), GWB, and PPR in 2011 are used. The cross river resolution of the mesh upstream of Poughkeepsie is very small as Hudson River becomes much narrower. This sets a very strict constraint on time step for transport modeling. To enhance the efficiency of the model with the objective for long term morphological simulation, salinity and sediment modeling uses only the mesh downstream of Poughkeepsie where the maximum salinity wedge infrequently reaches, with the water level boundary condition obtained from the LHR hydrodynamic model. This also takes the advantage of sediment load data available at Poughkeepsie and avoids unnecessary calibrations of sediment transport upstream of Poughkeepsie.

Simulated and observed salinity time series at three locations are shown in Figure 16, which agrees with each other pretty well. The NS coefficient is not calculated as there are some missing data in the observation. It should be noted that salinity has no impact on hydrodynamic results and a minor (less than first order) impact on sediment transport.

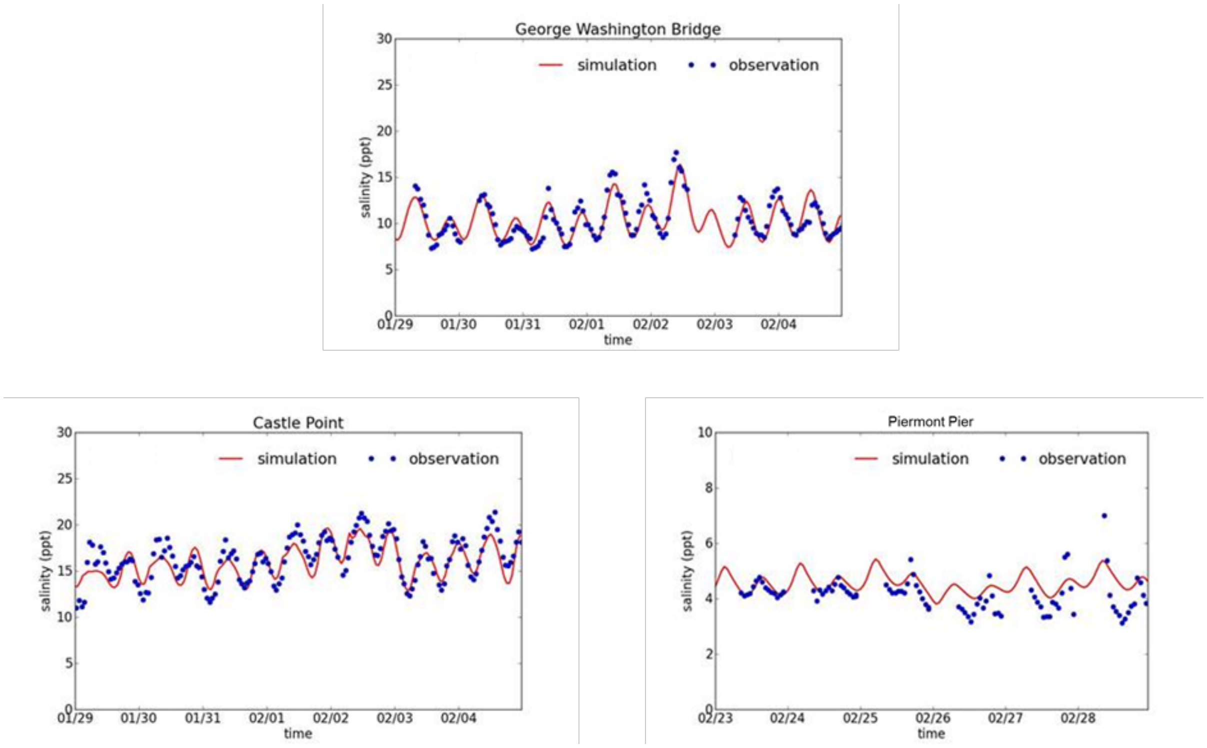

Figure 16: Comparison of Simulated Salinity Results and Observations for a Segment of the Jan–Mar 2011 Simulations. (top) CPT (bottom left) GWB and (bottom right) PPR

5.0 HOH MODEL DEVELOPMENT

The smaller and more refined HOH Model was created to resolve the geometry with higher resolution specifically around the Site as compared to the larger LHR Model. This HOH Model is such that there are approximately 29 grid cells along the Site. This allows for approximating shear stresses along the bed near the Site in the area of interest. Further, this HOH Model can be used to generate boundary conditions for very fine/highly resolved models at specific locations along the site to address more detailed design questions for different Site alternatives.

To support the finer mesh, the bathymetry/topography data used for the HOH Model was more highly resolved. The model utilized the available sources of data in each area of coverage. The LHR model resampled the resulting topo/bathy to 50m whereas the HOH model utilized 7 m resolution in the vicinity of the Site and 25m further upstream/downstream and offshore. Compared to the LHR Model, the HOH Model includes detailed LiDAR at the Site to assess forcing conditions during flood stage. The length of HOH Model mesh is about 6500 m with the Site centrally located along the eastern bank. The HOH Model mesh possesses 122 and 46 nodes along the river and across the river, respectively; where the density of cells increases locally to produce ~25 m by ~25 m cells around the Site (See Figure 17 and Figure 18).

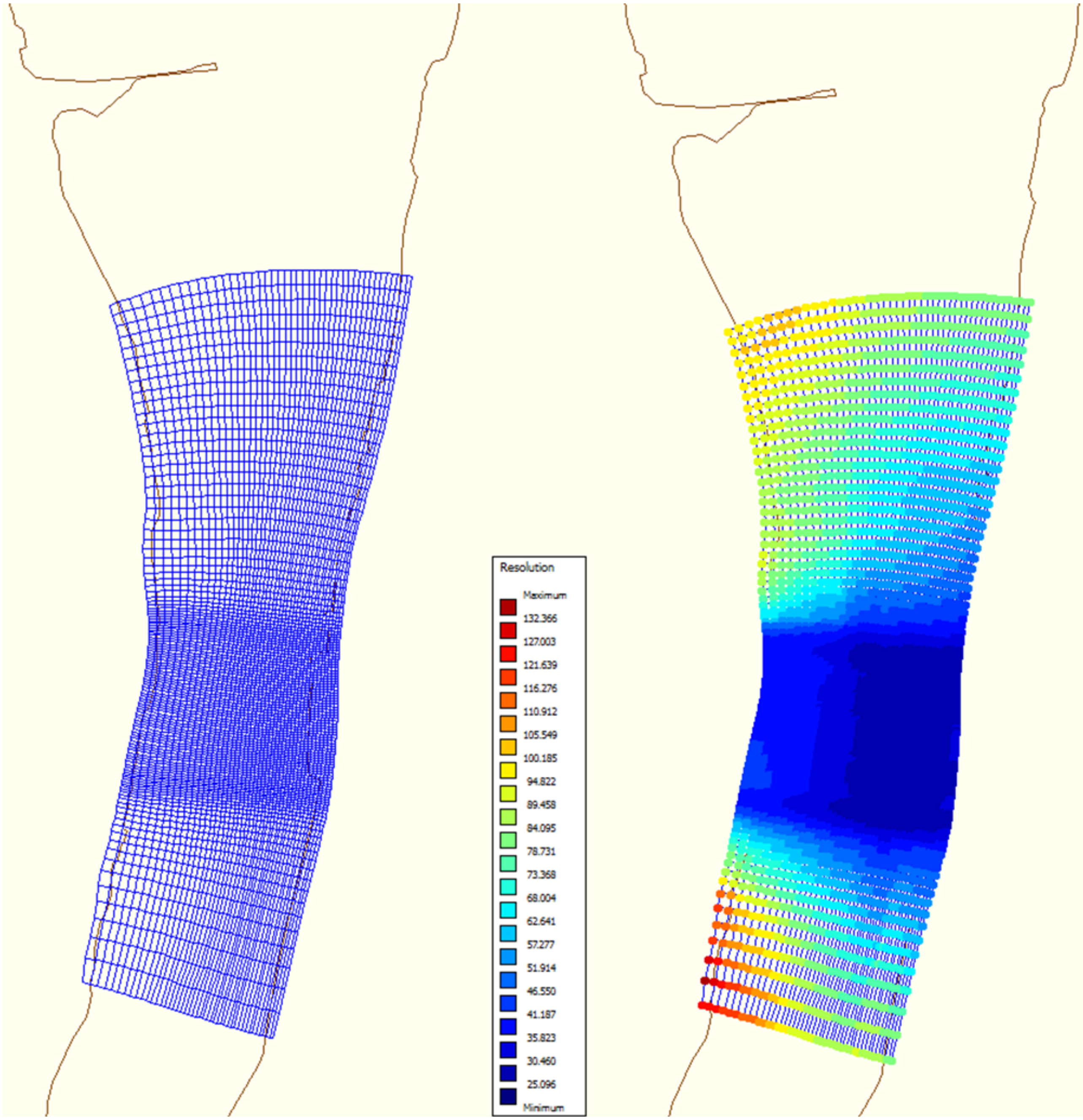

Figure 17: (left) HOH Mesh Coverage (right) HOH Mesh Resolution

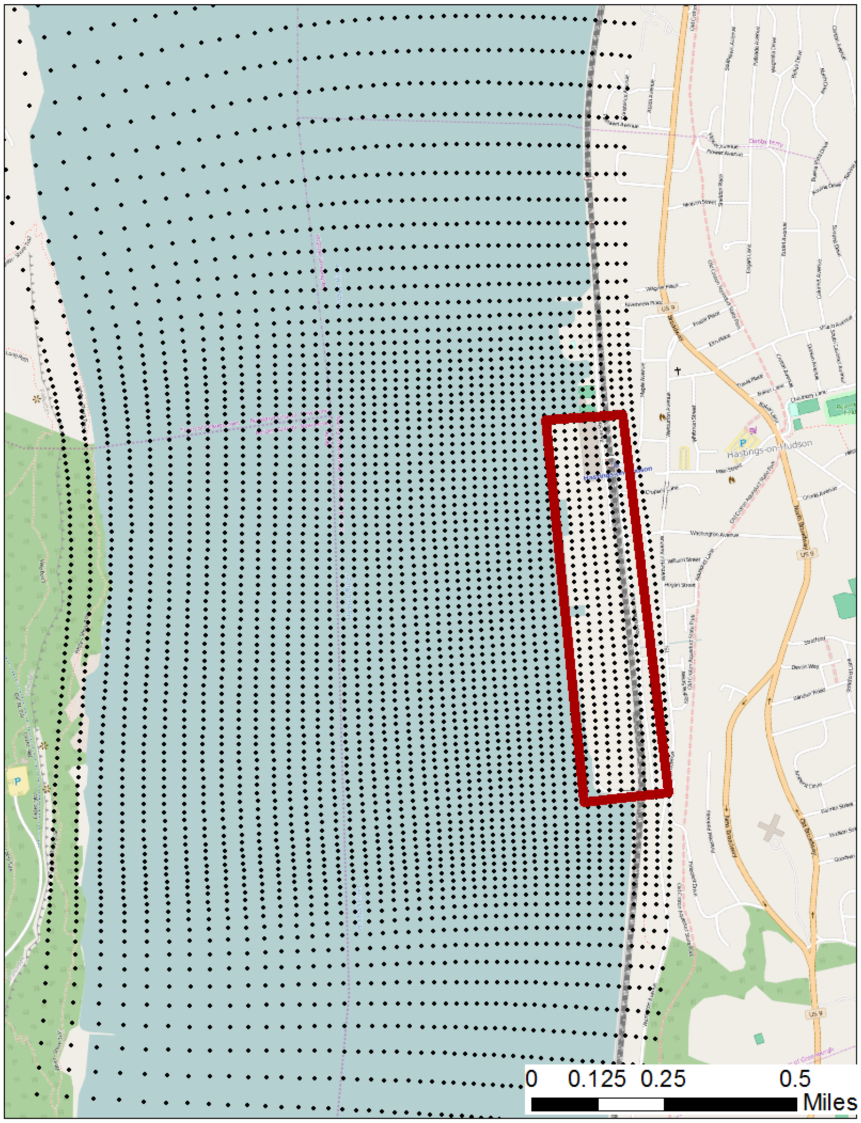

Figure 18: Mesh Coverage near the Site (Outlined in Red)

Water levels at the downstream boundary condition and the depth averaged velocity at four segments on the upstream boundary were imported from LHR Model. Since the depth averaged velocity is variable across the river, four segments (Velocity 1–4) were chosen at the upstream boundary to resolve the velocity variation along the boundary (See Figure 19). Salinity was not taken into this validation process as the salinity variation within the HOH Model domain is minimal and will have no impact on the hydrodynamics. With the exception of time steps, physical parameters, and numerical settings were exactly the same as those applied in LHR Model. The time step in LHR model was 1 minute while it was 0.03 minutes in the HOH Model to account for the fact that the minimum cell size is smaller than that of LHR model.

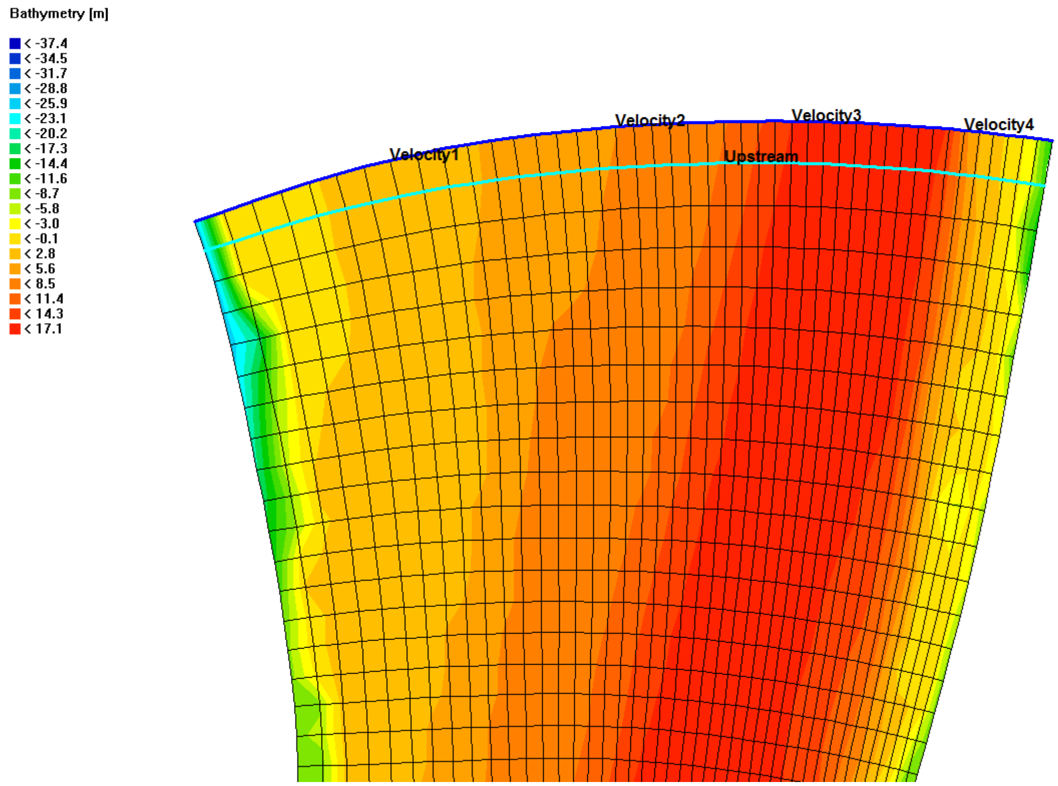

Figure 19: Upstream portion of the HOH Model with velocity boundary conditions

Those nodes on the boundary in which the water level is defined should be always either wet or dry otherwise numerical instability is produced at the boundary and transported through the entire domain. Therefore, the depth was decreased or increased slightly so that nodes at the downstream boundary are always only wet or only dry, respectively.

Three observation points were defined in both the LHR and HOH Model to compare water level and depth averaged velocity vectors. Figure 20 shows these locations where model-to-model validation was performed.

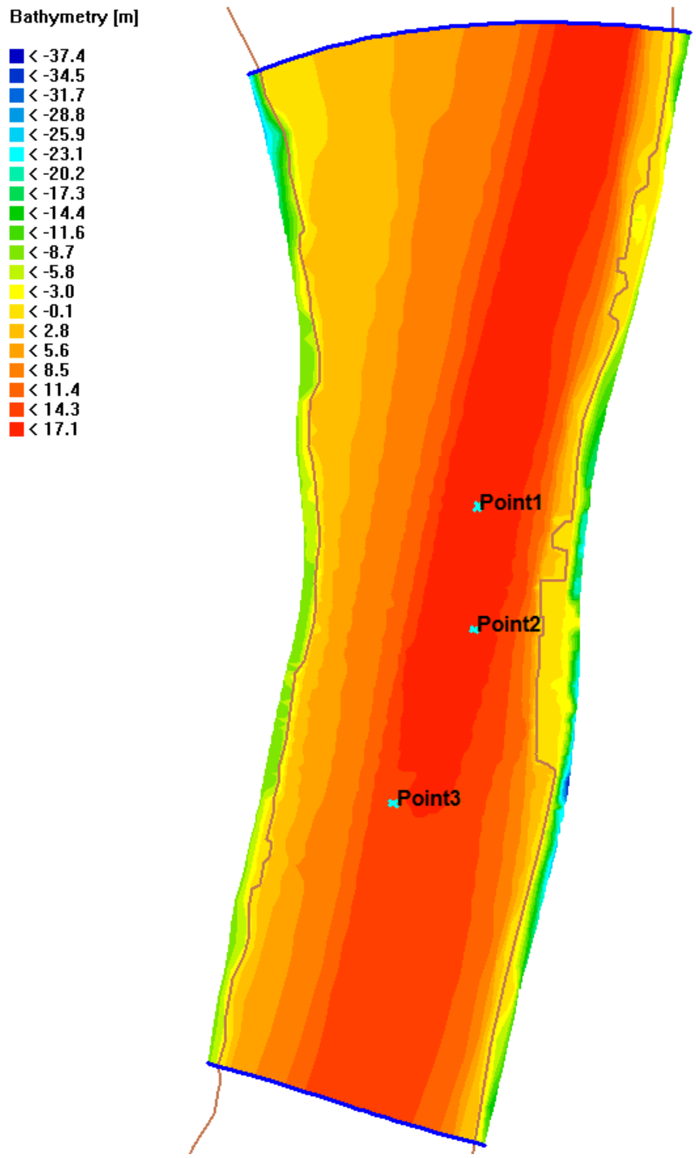

Figure 20: Location of observation points for model-to-model validation

The water level and depth averaged velocity vector at these observation points for the first two weeks of June 2005 from LHR and HOH Models are compared in Figure 21 and Figure 22. In these figures the blue color represents the HOH Model and the red color represents the LHR Model. Results show that the HOH Model can reproduce the LHR Model very well and the LHR and HOH Model results are very similar, indicating strong agreement between these two models. Since the LHR Model has been calibrated and validated against observations, the fact that the HOH Model matches the LHR indicates that the HOH Model is similarly calibrated and validated. In terms of performance, the HOH Model simulations take roughly the same amount of time (0.13 hrs/day) as the LHR Model, which was deemed to be an acceptable speed for long-term simulations.

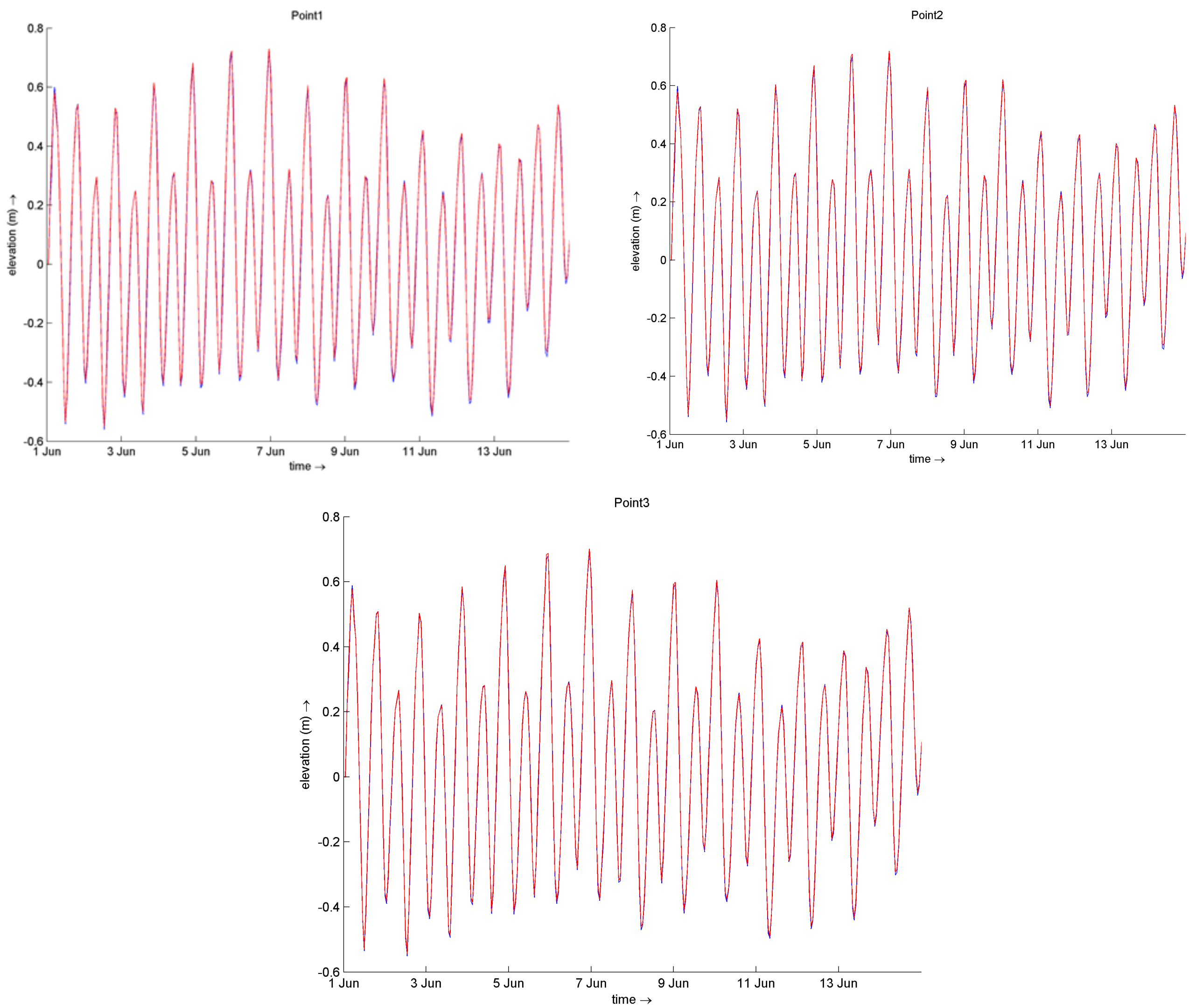

Figure 21: Water level at the three observation points for model-to-model validation, HOH (blue) versus LHR (red)

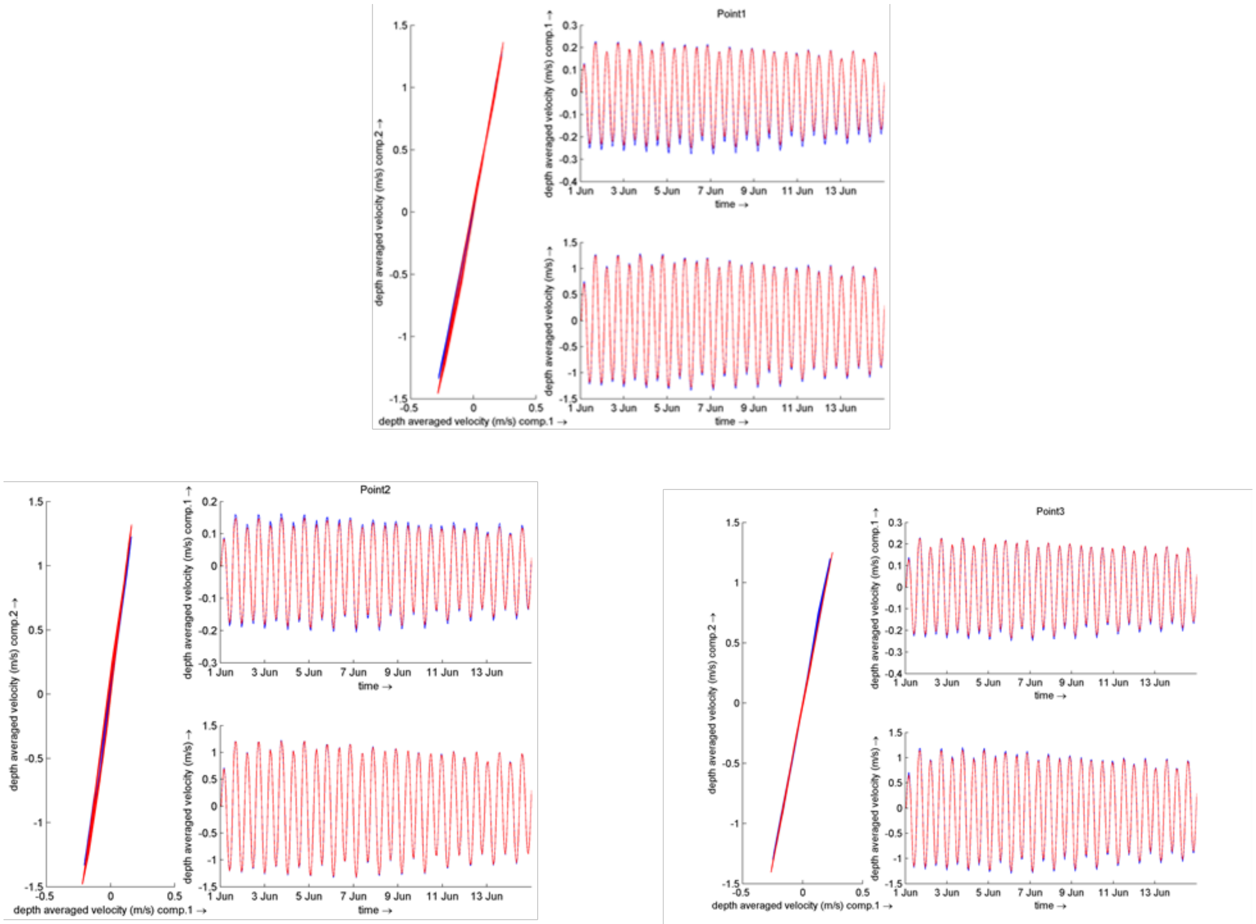

Figure 22: Depth averaged velocity at the three model-to-model observation points, HOH (blue) versus LHR (red)

6.0 PROPOSED SEASONAL AND EXTREME FORCING CONDITIONS

Making any alterations in a river or estuary and along its coast may affect prevailing morphodynamic trends within the vicinity of these alterations. It may be of interest to investigate this change in trends to answer questions regarding long term erosion/deposition patterns near the Site. These alterations can be thought of as perturbations to an otherwise quasi-steady system. Following this 'perturbation,' it may take years or decades to yield morphodynamic trends that are in quasi-equilibrium with prevailing forces. Since it is unlikely that a historical set of years will repeat itself in the future, using hindcast (a history of observation) to forecast long term morphology should be avoided if a better alternative exists.

One such alternative is to forecast a 'synthetic' year rather than selecting a year from the historical record to investigate forces at the Site and morphodynamic changes resulting from Site activities. By performing a statistical analysis of the water levels at The Battery and discharge at Green Island, synthetic annual time series of these boundary conditions have been created for long term simulation. Since water levels and discharge have strong seasonal dependence, the approach taken is to derive monthly statistics for these variables, from which monthly time series can be selected. These selected months can be combined to create a synthetic year for modeling purposes. The remainder of this section describes the statistical analysis and methodology to create synthetic annual time series that can be adjusted to include more occurrences of strong storms or, conversely, controlled to reduce the likelihood of strong conditions.

6.1 WATER LEVEL

Based on the initial LHR Model simulations, the main contributor to modeled water levels and current velocities near the Site is water level variations at the model downstream boundary located at The Battery. The water level variations include astronomical tides and a residual component, or surge, induced by wind and atmospheric conditions, which account for the variable nature of water levels that deviate from predictable tides. This surge component was separated from the water level at The Battery using a harmonic analysis of observed water level from 1980 to 2015 and is plotted in Figure 23. The figure shows that both positive and negative surges affect water level at this location with the highest residual water level corresponding to Hurricane Sandy in late October 2012 (about 2.8 m above the tidal level).

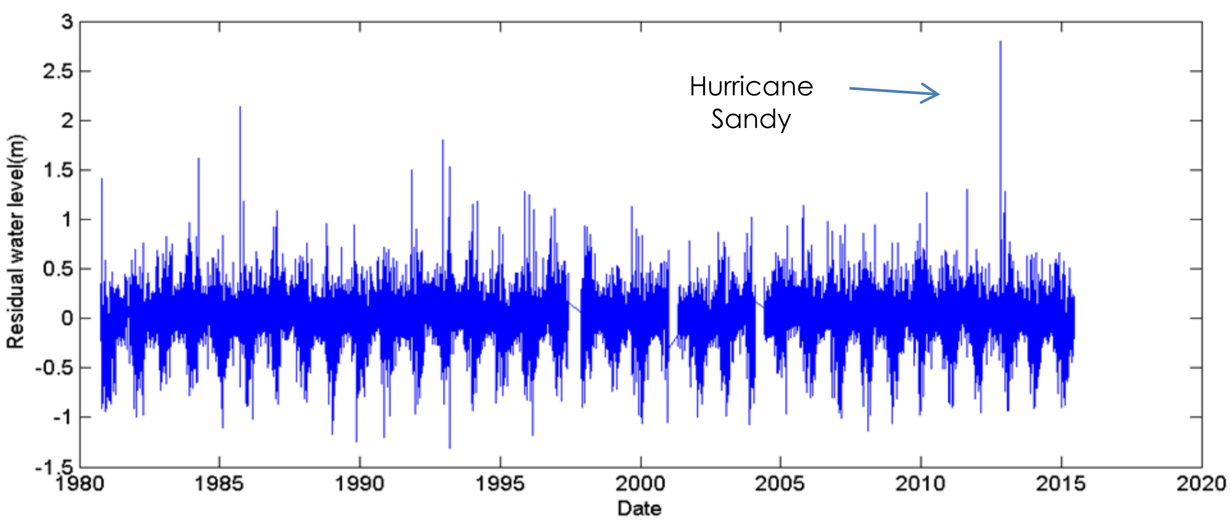

Figure 23: Residual component of the water level (surge) at The Battery from 1980 to present

As previously mentioned, the surge component arises from local wind and pressure fields. Winds vary in magnitude and direction in short periods of time (i.e., minutes) but these magnitudes and directions are biased by slower moving atmospheric conditions (i.e., pressure fields and storms). This short period variation accounts for the noise when analyzing a time series of residual water level. The longer period or lower frequency signal of the time series represents the passing of pressure fields. Figure 24 shows an example month in which this high frequency noise and lower frequency trends can be observed.

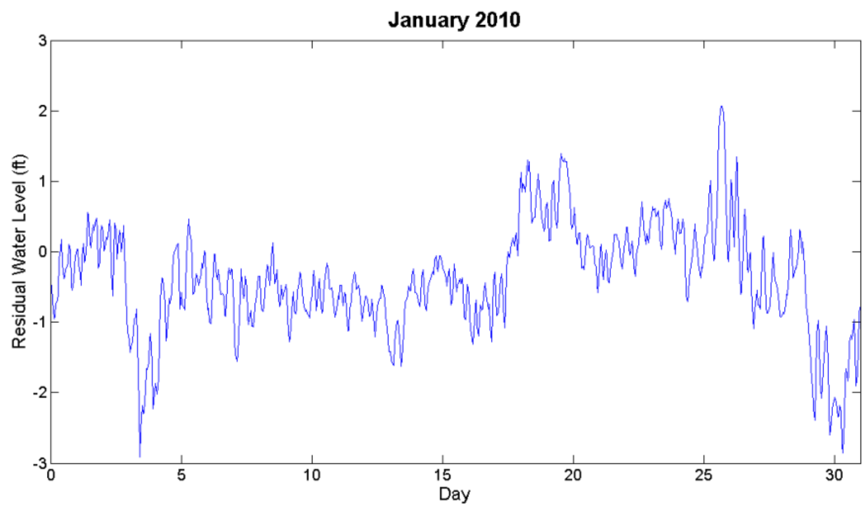

Figure 24: Residual water level at The Battery during January of 2010

Hourly water levels recorded at The Battery were obtained from November 1926 to the end of 2013. From this data record, the residual water level was extracted using the WORLD TIDES application in MATLAB®. The residual water level was separated by each of the 12 months. Initial attempts were made to utilize monte carlo methods with monthly statistics to achieve synthetic residual water level time series for each month. However, methods to superimpose trend lines on statistically determine random values poorly represented the general qualitative trends of actual residual water levels. Therefore, this approach was abandoned in favor of selecting actual records to create a synthetic year from a composite of observations.

Since the synthetic time series is necessary strictly for addressing questions pertaining to long term morphology trends (deposition/erosion patterns, achievement of equilibrium bathymetry post disturbance, etc.) it should represent the most likely conditions. Furthermore, it should exclude extreme events (i.e., strong positive and/or negative surges) since these can be superimposed on the synthetic time series to investigate a given year with an extreme event. In order to select the most representative year for each of the 12 months, the maximum positive and negative surges (maximum and minimum residual water levels) for each month and year combination was retained. Any month and year combination for which there was not a complete record of water levels (e.g., when the gage failed to collect data) were removed from the analysis.

For each month, the average maximum positive and negative surges were computed and these averages were compared to each year's value. For each month, the years were ranked based on these comparisons. The year with the best combined ranking for positive and negative surges was selected for each month. The time series of residual water levels for these month/year combinations were obtained from the observed record and combined to create a synthetic year of residual water levels (Table 11). This synthetic annual residual water level time series was summed with the astronomical tide from 2010 as extracted from WORLD TIDES. The year for the astronomical tide was selected at random because astronomical tides are insensitive to the year selected, saved for the timing of high and low, as well as, spring and neap tides. This summation provides a water level time series for baseline annual model.

Table 11: List of Selected Years for Baseline Water Level Time Series

Month	Year	Month	Year
1	1941	7	1962
2	1952	8	1946
3	1945	9	1948
4	1991	10	2013
5	1994	11	1993
6	1929	12	2005

As previously mentioned, this method to concatenate representative months to establish a synthetic year excludes extreme events. The rationale is to maintain the ability to model average conditions for longer term simulations. However, the impact of severe events can be assessed by simply super-imposing those extreme water levels onto the baseline time series. The NOAA-determined annual-percent-chance water levels (tide plus residual) at The Battery are presented in Table 12. It should be noted that Hurricane Sandy produced water levels more than 1 m above the 1%-annual-chance (100-year) water level and this water level has been closely reached over the past 50 years by the dates and months listed. Once design guidance is provided from the design engineers, storm events from historical observations or synthetic storms exceeding the strength of historic storms can be hindcast/simulated to obtain extreme shear stresses for structural design andsuperimposed in the baseline year to see the difference between an average year and one with major storm(s).

Table 12: NOAA's Predicted Extreme Water Levels at The Battery compared with Extreme Events in the Record

Percent Annual Chance	High Water Level (m, NAVD88)	Low Water Level (m, NAVD)
1%	2.44	-1.89
10%	1.86	-1.71
50%	1.49	-1.49
99%	1.22	-1.16
Recorded		
Sandy	*3.50*	---
September 1960	*2.33*	---
December 1992	*2.24*	---
August 2011	*2.15*	---

A comparison has been made between the synthetic year and the observed water level during 1953, which was selected because its average monthly peak positive and negative residual water levels were closest to annual averages. The plots in Figure 26 show a comparison between the synthetic water level and the observations during 1953 over the last 65 days of the year (fall) and days 90–150 (spring). The limit of the y-axis in either plot indicates the 10%-annual-chance high and low water values; neither time series exceeds this value. This is desirable because the 10%-annual-chance values have a 1% chance of occurring on consecutive years so events of this magnitude or greater ought to be imposed on the synthetic year for multiyear simulations with 'storms.' The baseline year exceeds the 99%- and 50%-annual-chance high water values on 101 and 4 occurrences, respectively (1902 and 2 occurrences in 2010). The 99%- and 50%-annual-chance low water values are exceeded on 3 and 0 occurrences as opposed to 10 and 0 in 2003. It is desirable to achieve at least the 99%-annual-chance values since there is a 90% chance of these values being exceeded in 10 consecutive years.

Theoretically, exceeding the 50%-annual-chance value in the synthetic year may be undesirable since the probability of exceedance in a consecutive year drops below 10% after 3 years. However, the fact that the 50%-annual-chance high water is exceeded in the synthetic record is of little concern because the empirical record indicates that NOAA's estimation of the 99%- and 50%-annual-chance high water values are too low. This is demonstrated by the fact that the positive residual water levels are exceeded on numerous occurrences in a given year. Considering all factors, the synthetic annual water level time series excludes water levels that are unlikely to occur in consecutive years without being too conservative and excluding high probability exceedance values.

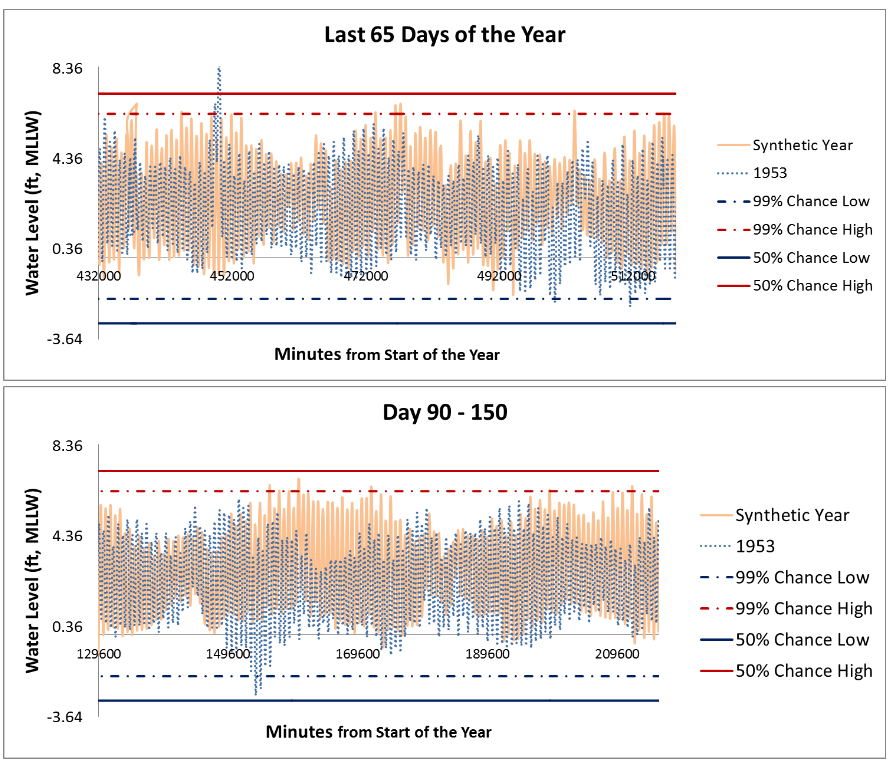

Figure 25: Comparison between the synthetic water level and observations

Another consideration for assessing extreme forces for structural design is the potential for strong waves coincident with high water levels to impact the Site. The preliminary flood insurance study and associated modeling for Westchester County shows the presence of wave induced high hazard zones (VE-zones) along the Site with a 1%-annual-chance (100-Year) wave height and period of 1.16m and 3.82s, respectively. The return period water levels at the Site as computed in the preliminary flood insurance study as well as the water level measured at the USGS station near the Site in 2011 are presented in Table 13.

Table 13: Water Level Recurrence Intervals at the Site from the Preliminary Flood Insurance Study Compared with Measured Data on August 2011

Percent Annual Chance	Water Level (m, NAVD88)
0.2%	3.52
1%	2.56
2%	2.23
10%	1.56
August 2011	*2.25*

As previously mentioned, modeling extreme events can be performed rapidly since the modeling time frame is short (only hours or days). Therefore, simulations can be performed on demand to assess hydrodynamic conditions from historic observations or synthetic more extreme storms, and can include/exclude estimated wave forcing from historic or synthetic winds.

6.2 DISCHARGE

An initial test of sensitivity to discharge was performed by running multiple short term simulations with constant discharge at the upstream. More specifically, model simulations with steady discharge at Poughkeepsie of 0, 200, 500, 750, 1000, 1500, 2000 m^3/s were conducted. The percent difference between the magnitudes of peak depth averaged velocities relative to 0 m^3/s steady flow scenario are as follows: 1.5%, 3.7%, 5.5%, 7.3%, 11.0%, and 14.8% for 200, 500, 750, 1000, and 2000 m^3/s, respectively. Though peak discharges due to severe rainfall events or snow melt exceed the tested range, it should be noted that the base flow of the Hudson River is less than 200 m^3/s while the tidal flux at Battery is about 13,000 m^3/s (Henshaw 2011). Therefore, river discharge was completely excluded; there would be negligible impact on hydrodynamic results at the site. However, stronger discharge events are likely to have detectable impacts on hydrodynamics at the Site. Therefore, it is similarly important to develop a synthetic annual hydrograph for river discharge that includes events that are likely to occur in consecutive years.

As a first step, the base flow and storm runoff were separated from one another using a program called HYDSEP developed by the USGS. The average base flows, maximum peak storm runoff, and total storm runoff volume (integrating under the storm runoff time series) were calculated for each month. For each month, the average base flow for that particular month over the entire observed record was applied (1946–2015). Similar to the water level analysis, any month that was incomplete owing to data gaps was excluded. Rather than applying the base flow uniformly across each respective month, the average baseflow was applied at the middle of each month and interpolated. This avoided a discontinuous 'stairstep' base flow time series (Figure 26, top).

Storm flows were analyzed to select a year for each month that had relatively calm (excluding atypically calm years) flows by a process similar to that used in selected residual water levels. To do so, the average peak flow and average storm runuoff volume over the entire observed record was computed for each month. The year whose peak flow and runoff volume were closest to the averages were identified for each month. An annual time series of storm flow was created by concatenating these monthly storm flow time series for these identified years. The base flow time series was summed with the concatenated monthly storm flow time series to yield a synthetic annual total flow time series (Figure 26, bottom).

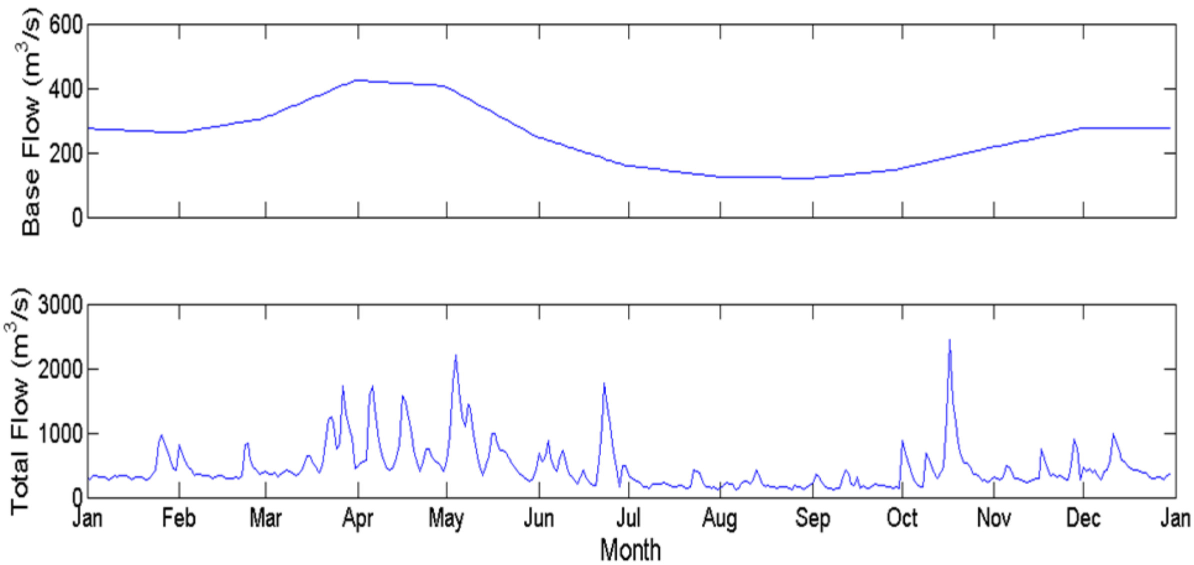

Figure 26: (top) Annual base flow derived from monthly averages (bottom) Annual total flow time series derived from average monthly base flow and storm flow from selected years

7.0 REFERENCES

Abood,K.A, G.A. Apicella, and A.W. Wells. 1992. General evaluation of Hudson River Freshwater Flow Trends. In *The Hudson River Environmental society*, Estuarine Research in the 1980s, Edited by Smith, C.L

Ding, Y. and S.Y. Wang. 2006. Development and validation of integrated coastal process models for simulating hydrodynamics and morphological processes, US-China workshop on advanced computational modeling in hydroscience and engineering, Oxford USA.

Earth Tech. 2003. OU-2 Feasibility Study for Hasting on Hudson, correspondence from Ryan Scott, November 19, 2015, Haley & Aldrich of New York, 200 Town Centre Drive | Suite 2, Rochester, NY 14623.

Henshaw, R.E. 2011. Environmental History of the Hudson River: Human Uses that Changed the Ecology, Ecology that Changed Human Uses. SUNY Press USA.

Nitsche, F.O., W.B.F. Ryan, S.M. Carbotte, A. Slagle, C. Bertinado, R. Flood, T. Kenna, and C. McHugh. 2007. Regional patterns and local variations of sediment distribution in the Hudson River Estuary, Estuarine, Coastal and Shelf Sci Vol 71, 259-277.

Ralston, D.K., W.R. Geyer, and J.A. Lerczak. 2008. Subtidal Salinity and Velocity in the Hudson River Estuary: Observations and Modeling, J Phys Oceano, Vol 38, 753-770.

Ralston, D.K., W.R. Geyer, and J.C. Warner. 2012. Bathymetric controls on sediment transport in the Hudson River estuary: Lateral asymmetry and frontal trapping, J Geophys Res Vol 117.

Wang H.V., J.D. Loftis, Z. Liu, D. Forrest, and J. Zhang. 2014. The Storm Surge and Sub-Grid Inundation Modeling in New York City during Hurricane Sandy. J. Mar. Sci. Eng. 2014, 2, 226-246; doi:10.3390/jmse2010226.